A NEW VARIABLE SHEAR CAPILLARY VISCOMETER

A NEW DESIGN FOR A CAPILLARY VISCOMETER, FOR MEASUREMENTS OF NON-NEWTONIAN FLOW OF DILUTE POLYMER SOLUTIONS

by

HENK VAN OENE, chem. cand.

A Thesis

Submitted to the Faculty of Graduate Studies

in partial fulfillment of the requirements

for the degree

Master of Science

McMaster University

October 1958

Aan Mevrouw D. J. Stormink-Loozeman

MASTER OF SCIENCE (1958) McMASTER UNIVERSITY

(Chemistry) Hamilton, Ontario

TITLE: A new design for a capillary viscometer, for measurements of non-Newtonian flow of dilute polymer solutions.

AUTHOR: Henk van Oene, chem. cand. (State University of Groningen, The Netherlands)

SUPERVISOR: Professor L. H. Cragg

NUMBER OF PAGES:

SCOPE AND CONTENTS: The theory and measurement of non-Newtonian flow in capillary viscometers is reviewed, and criteria for variable shear capillary viscometers have been given. Three modifications of the Ubbelohde viscometer have been designed to meet these criteria. These viscometers have been used in viscometric measurements with three different non-Newtonian polymer-solvent systems. Their performance, and the results obtained with them, are discussed.

ACKNOWLEDGEMENTS

The helpful discussions and encouragement of Professor L. H. Cragg, under whose supervision this work was done, is gratefully acknowledged.

Thanks are also due to Dr. J. A. Manson and Dr. C. C. Bigelow for their introduction of the author to Canada.

The aid of Messrs. D. Smith, A. Edgar and A. Tapajna as summer assistants is very much appreciated.

The author is very grateful to Dr. Allene Jeanes and Dr. S. N. Chinai for making available suitable fractions of Dextran and poly(n-octylmethacrylate), used in this investigation.

The financial aid from the Defence Research Board and the National Research Council in the form of grants-in-aid, and of the Department of Chemistry in the form of term scholarships, have contributed much to the completion of this project.

H. van Oene.

ABSTRACT

Since Newton's definition of viscosity does not lead to a useful description of non-Newtonian flow, two other model liquids, the Maxwell liquid and the Prandtl-Eyring liquid are discussed. Equations describing the flow behaviour of these liquids in narrow capillaries are derived and discussed.

A thorough analysis is given of corrections that are, or may be, necessary in capillary viscometry, and the influence of non-Newtonian flow on these corrections is discussed, both for cylindrical and spherical bulbs.

The significance of measurements of non-Newtonian flow in dilute solutions of macromolecules is discussed in terms of recent theories. It is shown that a capillary viscometer has inherent limitations for such measurements, but that a properly designed capillary viscometer can give precise and reliable data at shear rates down to 50 sec^{-1}, provided that the system is not too shear-dependent.

A new variable shear capillary viscometer--a modification of the Ubbelohde suspended level viscometer--is described. It was designed to be rugged, convenient and precise, to eliminate or minimize the kinetic energy correction and surface tension effects, and to permit dilution of a solution while in the instrument. Three different viscometers

of this type have been constructed, calibrated and tested, and proved sound in design and convenient in use.

The usefulness of the viscometers has been demonstrated in three diverse investigations: (i) the shear dependence in aqueous solutions of a high molecular weight dextran, (ii) the temperature dependence of the zero-shear intrinsic viscosity in a good solvent of a very high molecular weight fraction of polystyrene, (iii) the shear dependence of the interaction coefficient k' in the systems polystyrene-toluene and poly(n-octyl-methacrylate).

TABLE OF CONTENTS

LIST OF TABLES

LIST OF FIGURES

INTRODUCTION

The measurement of the dependence on driving pressure of the viscosity of a dilute polymer solution, when flowing through a narrow capillary, has received more and more attention in recent years.

Until about 1950 this effect was almost completely ignored. Even now thorough and precise investigations are still lacking. The most complete investigation is still that carried out in this laboratory by Sharman (58) and Sones (61), using a range of polystyrene fractions and a variety of solvents at several different temperatures. Although this was an extensive rather than an intensive investigation, the results have been widely used to test various theories that have been developed (8, 28, 47, 74). The reason for the paucity of studies of shear dependence of viscosity is that this is exhibited only in systems in which the polymer molecules are stiff, or flexible and very large (molecular weight $> 10^6$). These polymers have only recently become objects of scientific interest. Now they are of great interest indeed.

On the basis of the various theories proposed to account for the shear dependence of the viscosity, it became

evident that measurements should be made at extremely low driving pressures, since the quantity of interest is the limiting viscosity at zero shear stress. The results of the early experiments were in flat contradiction with the predictions of theory, which requires a quadratic dependence on the shear stress to account for the fact that the viscosity of a liquid does not depend on the direction of flow. In early experiments a linear dependence was found in the lower shear stress range. Gradually it was realised that the measurements had not been extended to sufficiently low shear stresses. In order to make these measurements it was necessary to modify the technique or, better, the viscometers, to permit applying a very low, steady pressure. Little or no attention has been paid in these adaptations to the question whether or not the viscometer used was able to give meaningful data in this very low range of shear stresses.

It was, therefore, decided to make a thorough study of the viscometry of non-Newtonian liquids at low driving pressures (particularly in capillary viscometers) and try to develop a capillary viscometer, capable of giving precise reliable data at very low driving pressures. This thesis, then, is concerned with the conclusions drawn from and prompted by a thorough review of the literature, with the designing of a variable shear viscometer, and with its testing and use in typical studies of the flow behaviour of dilute solutions of high polymers.

Chapter I

DEFINITION AND MEASUREMENT OF THE COEFFICIENT OF VISCOSITY

A. Definition of Viscosity and Poiseuille's Equation

1. Newton's Definition of Viscosity. The first definition of viscosity is due to Newton. He considered the following case:

A volume of liquid is sheared between two parallel plates of area f, which are separated by a distance x. The velocity of one plate relative to that of the other is v. Then the force resisting the relative motion of two adjacent layers in the liquid between the plates, can be expressed as

$$F = \eta \frac{dv}{dx} \cdot f \qquad (I - 1a)$$

$\frac{dv}{dx}$: velocity gradient in a direction normal to the direction of flow

η: coefficient of viscosity

F/f represents a shearing stress. Rearranged (I - 1a) becomes

$$F/f = \eta\, dv/dx \qquad (I - 1b)$$

This may be rewritten in the form

$$\tau = \eta q \qquad (I - 1c)$$

τ: shear stress

q: shear rate, or shear gradient

The coefficient of viscosity is thus defined as the ratio of the shear stress to the shear rate. It represents

a meaningful physical property of the liquid only, if this ratio remains constant for varying shear stress or shear rate. Liquids in which η, thus defined, is constant are called Newtonian liquids, those in which η varies, non-Newtonian liquids.

Since this definition is not based on any theory of flow, it is of no help in understanding why some liquids are Newtonian and others are not. In order to arrive at a more useful definition of viscosity, we must make some assumptions about the mechanism of flow. We will briefly outline two quite different descriptions of flow, that lead to more adequate definitions. One is due to Maxwell, who considers flow to be analogous to the relaxation of stress in an elastic solid; the other is due to Eyring, who treats flow as a rate process.

2. Maxwell's Treatment of Viscosity (49). Let a distortion or strain e be produced in a body by displacement. A state of stress p is thus established. The relation between stress and strain can be expressed as

$$p = \epsilon e \qquad (I - 2)$$

ϵ: Modulus of elasticity

If no relaxation of the stress occurs, p will remain equal to ϵe and hence

$$\frac{dp}{dt} = \epsilon \frac{de}{dt} \qquad (I - 3)$$

If however relaxation does occur, p will tend to disappear at a rate dependent on the magnitude of p and proportional to p. Then (I - 3) becomes

$$\frac{dp}{dt} = \epsilon \frac{de}{dt} - \frac{p}{\chi} \qquad (I - 4)$$

χ: Constant, with dimensions of time

If we now consider a system in which the stress is maintained constant and in which, therefore, there is a continuing displacement or flow, ($dp/dt = 0$) therefore (I - 4) becomes

$$p = \epsilon \chi \frac{de}{dt} \qquad (I - 5)$$

This is the desired stress strain relationship.

We may therefore define the coefficient of viscosity as the product $\epsilon \chi$. In this product ϵ is the modulus of elasticity and χ is the relaxation time for the stress p, as can be easily derived from (I - 4). Equation (I - 5) is equivalent to equation (I - 1b), for $de/dt = dv/dt = q$, and $p = \tau$. Hence Maxwell's definition of the viscosity, as being the product of ϵ and χ, corresponds to Newton's.

If $\epsilon \chi$ remains constant with varying shear stress the liquid is Newtonian. If the liquid is Non-Newtonian it is because $\epsilon \chi$ does not remain constant, which is not inconceivable, since many "constants" are frequency dependent.

If equation (I - 4) is rearranged and, for convenience, rewritten using the notation adopted in this thesis for shear stress and shear rate (τ and q respectively), it becomes

$$q = \frac{\tau}{\eta} + \frac{1}{\epsilon}\frac{d\tau}{dt} \qquad (I - 6)$$

3. Eyring's Treatment of Viscosity (20). Eyring postulates that there is an irregular lattice structure in a liquid. In this lattice many equilibrium positions will be empty. Such a system, when subjected to stress, will be readily deformable. The assumption is that the molecules jump from one equilibrium position to another. As long as the stress acts on a body, jumps will be favoured along the direction of stress, and hence flow will occur.

Consider now such a system in which shear occurs along sets of parallel shear layers. Let λ_1 be the distance between the layers, λ the distance between two equilibrium positions in the direction of shear, λ_2 the distance between two neighbouring molecules and λ_3 the mean distance between two flowing particles in the moving layer in a direction perpendicular to the shear. Then the following expression for the shear rate can be obtained

$$q = \frac{\lambda}{\lambda_1} 2 k' \sinh \frac{\lambda \lambda_2 \lambda_3}{2 kT} \cdot f \qquad (I - 7)$$

f: shear force/area

k': rate constants for the jumps

with: $k' = K \frac{kT}{h} \exp(-\Delta F^*)$

ΔF^*: free energy of activation

If the viscosity is defined as the ratio of shear stress to shear rate, one obtains for the viscosity

$$\eta = \frac{\beta}{\alpha} \frac{\sinh^{-1} \beta . q}{\beta q} \qquad (I - 8) \qquad \alpha = \frac{\lambda \lambda_1 \lambda_2}{kT}$$

$$\beta = \left[\frac{\lambda}{\lambda_1} 2 k^2 \right]^{-1}$$

The properties of the hyperbolic sinefunctions are

$$\lim_{\beta q \to 0} \frac{\sinh^{-1} \beta q}{\beta q} = 1 \qquad \lim_{\beta q \to \infty} \frac{\sinh^{-1} \beta q}{\beta q} = 0$$

Therefore at very low stresses

$$\eta = \frac{\beta}{\alpha} \qquad (I - 9)$$

At the limit of low stresses, then, the viscosity is constant. The liquid is Newtonian.

In Chapter II we will indicate how non-Newtonian flow in dilute polymer solutions can be described in terms of this theory.

As early as 1929, Prandtl, proposed an equation of the same form as (I - 7), based on almost the same considerations, but without the introduction of an absolute rate for the basic flow process. Recently Weymann (73) has combined the two approaches and shown them to be complementary. Prandtl's equation is

$$q = C \sinh \tau / A \qquad (I - 10)$$

C, A: constants to be determined by experiment

which for low stresses reduces to

$$\eta = A/C \qquad (I - 11)$$

which is equivalent to (I - 9).

4. Derivation of Poiseuille's Equation. Since we will be concerned with flow in narrow capillaries, we will give the derivation of the necessary equations on the basis of all three treatments of flow. Even though the derivation of Poiseuille's equation for Newtonian flow can be found in many textbooks, we will still derive it in order to make explicit the assumptions involved.

Consider a cylinder of liquid with a radius r and length L. If in flow all energy is dissipated in overcoming the viscous resistance, we may write

$$\pi r^2 p - 2\pi r L \tau = 0 \qquad (I - 12)$$

This gives the following expression for the shear stress:

$$\tau = \frac{pr}{2L} \qquad (I - 13)$$

We can now calculate the velocity distribution across the capillary, in a liquid flowing through a capillary tube, if we assume the velocity at the wall of the cylindrical tube to be zero. The velocity of a cylindrical annulus of liquid of radius r is

$$v = \frac{p}{4\eta L}(R^2 - r^2) \qquad (I - 14)$$

R: radius of the capillary

The volume Q flowing per second through a cross-section of the tube is then

$$Q = 2\pi \int_0^R vrdr = \frac{\pi R^4 p}{8\eta L} \qquad (I - 15)$$

This rearranges to the familiar form of the Poiseuille equation

$$\eta = \frac{\pi R^4 p}{8 VL} \cdot t \qquad (I - 16)$$

where V is the volume of liquid flowing through a cross-section in t seconds.

Let us now consider all the assumptions that have been explicitly or implicitly made:

i) All energy is used to overcome the viscous resistance. (This is certainly not correct, for the liquid acquires kinetic energy. Moreover other possibilities of energy dissipation can occur, for example a decrease in the entropy of the solute when subjected to a shearing stress.)

ii) the flow is laminar (this is true for pure liquids in the range of shear stresses considered. It may, however, not be true for a dispersed system, in which, in flow, local turbulence may occur because of the rotation of the dispersed particles.)

iii) There is no slip at the wall.

iv) The fluid is incompressible.

v) The fluid will flow, when subjected to the smallest stress, the viscous resistance being proportional to the velocity gradient. Or, in other words, there is no "yield value".

5. Derivation of Poiseuille's Equation for a Maxwell Liquid [52]. If we assume steady laminar flow, a derivative with respect to time can be replaced by a derivative with respect to the direction of flow, multiplied by the velocity distribution perpendicular to the direction of flow, or

$$\frac{d}{dt} = \frac{\partial}{\partial X} \cdot v(x,r) \qquad (I - 17)$$

In a capillary we have for the shear stress

$$\tau = \frac{p'R}{2} \qquad (I - 18) \qquad p' = \frac{dp}{dx}$$

the x-axis points in the direction of flow

Substitution of (I - 17) and (I - 18) in (I - 6) and subsequent rearrangement gives

$$\frac{dv}{dr} = \frac{r}{2}\left[\frac{p'}{\eta} + \frac{p''}{\epsilon} \cdot v(x,r)\right] \qquad (I - 19) \qquad p'' = \frac{d^2p}{dx^2}$$

If we now assume the same velocity profile as in (I - 14), one obtains from (I - 19) on substitution

$$\frac{dv}{dr} = \frac{r}{2}\left[\frac{p'}{\eta} + \frac{p'p''}{4\eta\epsilon}(r^2 - R^2)\right]$$

This can also be expressed as

$$\frac{dv}{dr} = \frac{rp'}{2\eta} \exp\left[\frac{p''}{4\epsilon}(r^2 - R^2)\right] \qquad (I - 20)$$

We can now calculate Q in the same way as in Section 4.

$$Q = 2\pi\int_0^R vrdr = 2\pi\frac{p'}{p''}\frac{\epsilon}{\eta}\left[\frac{2\epsilon}{p''}\left(1 - \exp\left(-\frac{p''R^2}{4\epsilon}\right)\right) - \frac{R^2}{2}\right] \qquad (I - 21)$$

which gives, after expansion of the exponential,

$$Q = \frac{\pi R^4 p'}{8\eta}\left[1 - \frac{p''R^2\chi}{12\eta} \;\ldots\ldots\; \right] \qquad (I - 22) \qquad \chi: \text{relaxation time}$$

From (I - 22) it follows that, in principle, one could evaluate the second term if one knew the value of dp/dL. Equation (I - 22) could then be solved as an ordinary differential equation with respect to dp/dL.

6. Poiseuille's Equation for a Prandtl-Eyring Liquid (46).

This derivation is more exact than the one given above for the Maxwell liquid, since the velocity profile is not assumed to be parabolic, but is derived from the flow-law itself.

The velocity profile is calculated as follows. For a Prandtl-Eyring liquid the expression for the shear rate is

$$q = -\frac{dv}{dr} = C \sinh \frac{p'r}{2A} \qquad \tau = \frac{p'r}{2} \qquad p' = \frac{dp}{dL}$$

Hence

$$v(r) = \int_0^R dv = \frac{C}{\alpha}(\cosh \alpha R - \cosh \alpha r) \qquad (I - 23) \qquad \alpha = \frac{p'}{2A}$$

which is the desired expression for the velocity profile.

Q can now be calculated in the usual way

$$Q = 2\pi \int_0^R vrdr = \frac{2\pi C R^2}{\alpha}\left[\frac{1}{2}\cosh \alpha R - \frac{1}{2\alpha R}\sinh \alpha R + \frac{1}{\alpha^2 R^2}(\cosh \alpha R - 1)\right] \qquad (I - 24)$$

which may be written in a simpler fashion as

$$Q = \frac{\pi}{4} CR^3 \cdot a\varphi(a) \qquad a = \frac{Rp'}{2A}$$

$$\varphi(a) = 1 + \frac{a^2}{9} + \frac{a^4}{240}$$

Or

$$Q = \frac{\pi R^4 p'}{8} \frac{C}{A} \left[1 + \frac{R^2(p')^2}{36A^2} \quad \ldots\right] \qquad (I - 25)$$

7. Comparison of the Various Forms of the Poiseuille Equation.

We have given three different derivations of the Poiseuille equation based on three different conceptions of the flow of a liquid. It is instructive to compare them. For a Newtonian liquid we have

$$Q = \frac{\pi R^4 p}{8\eta L}$$

For a Maxwell liquid

$$Q = \frac{\pi R^4 p'}{8\eta} \left[1 - \frac{p'^2 R^2 k}{12\eta} \quad \ldots\right]$$

For a Prandtl-Eyring liquid

$$Q = \frac{\pi R^4 p'}{8} \frac{C}{A} \left[1 + \frac{R^2(p')^2}{36A^2} \quad \ldots\right]$$

Since we have shown already that for low shear stresses the Maxwell liquid and the Prandtl-Eyring liquid reduce to a Newtonian liquid, the equations are equivalent in the limit of zero shear stress. At finite shear stress, there is an interesting possibility of distinguishing between the different rheological models, if one could measure dp/dL. For a

Newtonian liquid dp/dL is constant and equal to p/L. This does not hold for the two other liquids discussed. In principle dp/dL should be measurable. In practice, however, its measurement is difficult, since it has to be performed in very narrow capillaries without disturbance of the flow itself. So far only Schultz-Grunow (62) has succeeded in measuring dp/dL, employing delicate straingauges. A similar type of viscometer is being developed at the National Bureau of Standards by Swindells (66). It would be a major advance if these techniques could be developed for liquids whose viscosity is in the centipoise range, since it would make measurements on Non-Newtonian systems more accurate and reliable and much easier to interpret.

8. Modifications of Poiseuille's Equation. In Section 4 we have listed the various assumptions made in the derivation of the Poiseuille equation. In order to be able to apply this equation to actual measurements, certain modifications of it have to be made as to take account of the kinetic energy imparted to the liquid, of wall effects, and of the possible existence of a yield value.

a) The kinetic energy effect. The kinetic energy imparted per second to the liquid can be expressed as

$$\int_0^R \frac{1}{2} m v^2 = \int_0^R \frac{1}{2}(d \cdot dQ)v^2 \qquad (I - 26)$$

d: density

After substitution of (I - 14) in (I - 26) and evaluation of dQ/dr, one obtains

$$\text{Kinetic energy/second} = \pi d\left[\frac{P}{4\eta L}\right]^3 \int_0^R r^3(R^2 - r^2)^2\, dr \qquad (I - 27)$$

which on subsequent integration gives

$$\text{Kinetic energy/sec.} = \pi d\left[\frac{P}{4\eta L}\right]^3 \frac{R^8}{8} = \left[\frac{\pi R^4 P}{8\eta L}\right]^3 \frac{d}{\pi^2 R^4} = Q^3 \frac{d}{\pi^2 R^4} \qquad (I - 28)$$

The work done per second in overcoming the viscous resistance is

$Q \times P_{eff.}$ $\qquad$ $P_{eff.}$ the effective driving pressure

If a pressure P was applied only a part of it, P_{eff}, is used to overcome the viscous resistance. The effective driving pressure then is calculated as the total applied pressure minus the "pressure" required to give the liquid kinetic energy,

$$P_{eff} = P - \frac{Q^2 d}{\pi^2 R^4} \qquad (I - 29)$$

P: total applied pressure

Substitution of P_{eff} in Poiseuille's equation gives

$$\left(P - \frac{Q^2 d}{\pi^2 R^4}\right) \pi R^4 = 8\eta QL$$

which can be rearranged to a more familiar form of the modified Poiseuille equation

$$\eta = \frac{\pi R^4 Pt}{8VL} - \frac{Vd}{8\pi L}\,\frac{1}{t} \qquad (I - 30(a))$$

In the evaluation of the kinetic energy correction, the effect of the shape of the capillary ends was neglected. Unfortunately this effect has not been calculated rigorously and instead is taken care of by the introduction of an empirical constant m

$$\eta = \frac{\pi R^4 Pt}{8VL} - m\frac{Vd}{8\pi L}\frac{1}{t} \qquad (I - 30(b))$$

The value of this constant must be determined by a calibration with liquids of known viscosity. (For capillaries with trumpet-shaped ends, the value of m has been found to be 1.12.)

Because of the uncertainty in the value of m , viscometers should be designed in such a way as to make the second term in (I - 30(b)) negligible.

b) Wall effects. The assumption that there is no slip at the wall is not always valid; moreover the wall may distort the flow pattern in the liquid adjacent to it.

When the flowing liquid is a solution of flexible macromolecules, the molecules may tend to draw away from the wall because the shear gradient is greater at the wall than in the body of the liquid. Hence the layer of liquid closest to the wall has essentially the viscosity of the pure solvent. The rate of flow of liquid through the tube will thus be greater than expected from its actual viscosity, since the flow at the wall depends on the local viscosity only ([14]). If this effect

occurs, it would be difficult to detect in a non-Newtonian liquid, since its viscosity decreases for increasing shear stress. The only way to determine whether or not a wall effect exists, is to compare the viscosity measured at the same shear stress in viscometers with capillaries of different radius. If the viscosity is the same, there is no wall effect. For stresses smaller than 10^2 dynes/cm^2 the wall effect can be neglected.

Anomalies may also arise from absorption of solute on the capillary wall. Absorption will result in a decrease of the radius and hence an increase in the viscosity. This effect is significant only if the radius is smaller than 0.025 cm.

c) The yield value. If the liquid exhibits a yield value, that is, if the liquid flows only after a stress of a certain magnitude has been applied, suitable corrections can be made, but they are rather cumbersome. We will not discuss these corrections, because the liquids we will be dealing with do not exhibit a yield value. For an exhaustive treatment of the yield value one is referred to Reiner's book Deformation and Flow.

B. Measurement of Viscosity in Capillary Viscometers

1. Types of Capillary Viscometers. We have seen that it is possible to determine the viscosity of a liquid by studying its flow behaviour in fine capillaries. Capillary viscometers may be divided into two classes, absolute viscometers and relative viscometers.

a) Absolute viscometers. From measurements made in these instruments the viscosity is calculated with the help of equation

$$\eta = \frac{\pi R^4 P t}{8VL} - \frac{mV}{8\pi L}\frac{1}{t}$$

The accuracy of such a determination depends on a precise knowledge of all instrument dimensions and a detailed theoretical description of the flow behaviour within the instrument. The absolute calibration of these instruments is very time consuming and exacting.

b) Relative viscometers. In these viscometers one compares the viscosity of a liquid with that of another liquid, the viscosity of which is accurately known. If these instruments are so designed as to make the kinetic energy correction negligible, the ratio of the flow times of the two liquids is equal to the ratio of their kinematic viscosities. (The kinematic viscosity is defined as the ratio of viscosity to the density, η/d.) The calibration of these viscometers is carried out with a liquid of known viscosity, which enables

one to calculate the apparatus constant: $\pi R^4 hg/8VL$.

It should be realised, however, that the ratio of the flow times does not represent the ratio of the kinematic viscosities of the two liquids if the flow behaviour of these liquids is not identical. (For example a Newtonian liquid and a non-Newtonian liquid, liquid in laminar flow and a liquid in turbulent flow, etc.) A detailed description of the many different kinds of viscometers is not necessary here. Most of the more useful viscometers are fully described in Barr's "Monograph on Viscometry".

Chapter II

NON-NEWTONIAN FLOW AND ITS INTERPRETATION

The flow of a non-Newtonian liquid is such that the coefficient of viscosity decreases when the liquid is subjected to increasing shear stress. The most obvious way to describe this behaviour mathematically is to express the viscosity, or rather its reciprocal, the fluidity, in a power series in either shear stress or shear rate. One may exclude the odd-power terms in this expansion, since clearly the viscosity of a liquid should not depend on its direction of flow. The following expression is thus obtained

$$\phi = \phi_o + \sum_{K=1}^{n} \alpha_{2K} q^{2k} \qquad \text{(II - 1)}$$

ϕ : fluidity
ϕ_o : fluidity at zero shear rate

This expression can be valid only at low shear stresses, since it does not indicate the experimentally observed constancy of the viscosity at high shear stresses. Reiner (49) therefore proposed, as the simplest algebraical expression for the observed flow behaviour, the following

$$\phi = \frac{\phi_o + \phi_o \, q^2/\alpha^2}{1 + q^2/\alpha^2} \qquad \text{(II - 2)}$$

This empirical equation fitted remarkably well the data

obtained by Reiner with rather concentrated solutions of rubber in toluene. The disadvantage of (II - 2) is that it has no theoretical basis; it summarises the flow behaviour but is of no help in interpreting it.

1. Theories of Non-Newtonian Flow. In the last ten years a number of theories have been proposed, on the basis of which an almost quantitative interpretation of non-Newtonian flow can be given in terms of the properties of the solute.

a) Theory of Kuhn and Kuhn and others. A theory limited to dilute solutions of polymer molecules is one that has been developed mainly by Kuhn and Kuhn (33), Peterlin (43), Bueche (8), Rouse (50), Kirkwood (29,30), Zimm (75) and Cerf (9.10).

The polymer molecule in solution is assumed to have a "shape resistance", closely related to the "inner viscosity" in the domain inside the polymer coil. This "inner viscosity" is a result of hydrodynamic interaction between segments of the molecule and restricted rotation of the segments around the valence bonds. It makes the molecule more or less rigid. In flow this rigidity prevents the molecule from being completely oriented in the direction of the shear stress. As the shear stress increases the molecule becomes more oriented, and hence offers less resistance to flow, (or in other words, it has a smaller viscosity).

During flow a hydrodynamic torque induces a rotation of the particle. As Bueche ([8]) has shown, this will lead to a periodic compression and dilation of the molecule. If the molecule were perfectly elastic this alternating compression and dilation would not involve a loss in energy. Since most molecules are not perfectly elastic a certain amount of energy will be dissipated in rotation and hence the viscosity will be greater. As the molecule becomes more and more oriented in the direction of flow at higher and higher shear stresses this effect becomes less and less and the viscosity decreases. In a perfectly flexible molecule the effect of deformation just compensates the effect of orientation and no shear dependence will be observed ([15]). In all other cases the effect of orientation outweighs the effect of deformation and hence a net decrease in the viscosity is observed.

This theory, and its modifications, all lead to a final equation for the dependence of the viscosity on the rate of shear of the form

$$\eta_{sp} = (\eta_{sp})_{q=0}\left[1 - \beta q^2 \quad \right] \qquad \text{(II - 3)}$$

The coefficient β is expressed in molecular parameters. For the exact form one should consult the original papers.

The expression arrived at for the intrinsic viscosity are of the form

$$\frac{[\eta]}{[\eta]_{q=0}} = 1 - \text{constant} \left[\frac{q\eta_0}{RT} M [\eta]_{q=0}\right]^2 \qquad (II - 4)$$

The quantity in brackets merely represents the ratio q/D_{rot}, where D_{rot} is the rotational diffusion coefficient. Since the rotational diffusion coefficient is inversely proportional to the viscosity of the solution, we can rewrite (II - 4) in terms of shear stress, as was first pointed out by J. Hermans Jr. (24)

$$\frac{[\eta]}{[\eta]_{\tau=0}} = 1 - \text{const.} \left[\frac{q}{D_{rot}}\right]^2 = 1 - \text{const.} \left[\frac{q\eta_0}{q}\right]^2 = 1 - \text{const.}\, \tau^2 \qquad (II - 5)$$

From this it is clear that intrinsic viscosities, and also specific viscosities, should be compared at constant shear <u>stress</u>, not at constant shear <u>rate</u>, as is the usual practice.

The theory as briefly outlined above applies only to extremely dilute solutions. In considering more concentrated solutions, one should also take into account inter-molecular interaction. For very concentrated solutions promising results have been obtained by Lodge (35), who assumes a network to be built up in the liquid, due to entanglements of the polymer molecules. The "average lifetime" of the network junctions is dependent on the shear stress. The problem in concentrated solutions is made simpler since the hydrodynamical interaction between the molecules can, to a first approximation, be ignored.

The point of departure in the theories described above

was the polymer molecule itself. One may take a different approach, and try to account for non-Newtonian flow on the basis of some more mechanistic concept of flow. We will outline two such theories, one by Eyring and Ree ([48]), on the basis of the "hole" theory of liquids, the other by Oldroyd and others ([41, 37]) on the basis of a generalised Maxwell liquid.

b) Theory based on the Eyring concept of flow. In Chapter I we have given the derivation of Eyring's expression for the coefficient of viscosity

$$\eta = \frac{\beta}{\alpha} \frac{\sinh^{-1} \beta q}{\beta q}$$

The flow of polymer molecules is described as a movement not of whole molecules but of parts of molecules, a group of segments. Such a group of segments is called a flow-unit. The size of a flow-unit depends on the degree of segmental cooperation, and this can be characterised by a certain relaxation time. The final equation is a series of hyperbolic sine functions, whose argument depends on the relaxation time, and hence on the segmental cooperation in flow within the molecule. Each flow-unit contributes one term to the series. The expression obtained is

$$\eta = \frac{X_1 \beta_1}{\alpha_1} + \frac{X_2 \beta_2}{\alpha_2} \frac{\sinh^{-1} (\beta_2 q)}{\beta_2 q} + \frac{X_3 \beta_3}{\alpha_3} \frac{\sinh^{-1} \beta_3 q}{\beta_3 q} \qquad \text{(II - 6)}$$

where: X_n : fractional area occupied on a shear surface occupied by the nth group

β : relaxation time

$$\alpha_n = \frac{\lambda\lambda_2\lambda_3}{\gamma_n}$$

γ_n = mean available energy in the n^{th} group

The first term represents a Newtonian unit, the solvent, the other terms represent the non-Newtonian units.

Equation (II - 6) expresses an astonishing variety of phenomena from plastic flow in metals or amorphous solids to non-Newtonian flow in centipoise liquids, and it does so with very good precision and consistency. The basic disadvantage of equation (II - 6) is the a priori impossibility of predicting how many flow units are required, and how they are related to the structure of the molecule. Since, as the number of flow units increases, the number of adjustable parameters also increases, the question arises as to whether or not the excellent fit obtained is fortuitous.

The intuitive model for liquid flow, as developed by Eyring, has been employed by Umstätter et al (71) and by Schurz (54-56) to give an interesting interpretation of the flow curve, which is a plot of log shear stress versus log shear rate.

Umstätter (71), has shown, that one can identify the shear rate which has the dimensions of a frequency, with the frequency of segmental jumps. Therefore, as the shear rate increases the frequency of the jumps increases also. The greater the shear rate, the faster the molecule is led by flow

to the place vacated shortly before by another molecule. Hence the disturbance of the flow becomes less and less; when the shear rate reaches the value at which a molecule is carried by the flow to the place that another molecule is just vacating, the changing of places occurs with the smallest possible disturbance. The frequency of place-exchange (segmental jumps) has become a natural frequency of the system. At this shear rate the change in viscosity with shear rate has its largest value. This will correspond to a point of inflection in the flow-curve. The point of inflection will depend only on the size of the structural elements in flow and the viscosity of the solvent. Since the size of the structural elements will depend on the molecular weight of the solute one should in principle be able to calculate the molecular weight from the measured point of inflection. This molecular weight will only represent the molecular weight of the solute if the solute molecule is the fundamental unit in flow, an assumption that seems to be valid when dealing with stiff molecules such as the celluloses. Only for cellulose and cellulose derivatives does this description seem to be useful and is substantiated by a large amount of experimental evidence, due mainly to Schurz (54,55) and Edelmann (18). It does not appear to be satisfactory for dilute solutions of flexible molecules, since these molecules presumably do not have a unique flow-unit.

Since the point of inflection occurs within a range of shear stresses readily obtainable in capillary viscometers, further investigation of the validity of this empirical treatment would be of great practical value. It would mean that, in order to characterise a stiff molecule, all one would have to do would be to measure its flow-curve.

c) Theory based on the generalised Maxwell concept of a liquid (41). As already indicated in Chapter I, flow can be treated as a deformation phenomenon. A certain stress induces a corresponding strain, and the problem is to find the most general stress strain relationship. In Newtonian flow, there is strict proportionality between the stress and the rate of deformation. In non-Newtonian flow, the proportionality constant--the viscosity--is found to depend on the stress. To a first approximation the rate of deformation may be expressed as a power series in the stress. Such a relationship is written down for each of the components of the rate of deformation and for each of the components of the stress. The question arises as to which coordinate system to choose, since the deformation is referred to the deformed state and the stress to the undeformed state. Which choice is the correct one is still not clear (37). Moreover even when the reference coordinate system is chosen, the transformation to this coordinate system is not unique, since the only requirement is that the resulting tensor should be symmetric, thus

leaving an arbitrary combination of scalar quantities undetermined. Nevertheless, some useful equations have been proposed; of these we will only mention the equation derived by Oldroyd (40) for a generalised Maxwell liquid

$$\tau + \lambda_1 \dot{\tau} = \eta_0(q + \lambda_2 \dot{q}) \qquad (II - 7)$$

λ_1, λ_2: relaxation times

This equation has been shown by Toms et al. (68), to represent the flow behaviour of not too concentrated solutions of poly(methylmethacrylate).

2. Summary. It has been shown that important information with respect to the structure of the molecule can be obtained from the measurement of non-Newtonian flow in dilute solutions of macromolecules. The required data can to a large extent be obtained by means of capillary viscometry, at least for stiff molecules.

With respect to the mechanism of non-Newtonian flow, no information can be obtained with the present technique of capillary viscometry, since this would require the measurement of dp/dL.

In order to establish criteria for the applicability of an equation of flow as the generalised Maxwell liquid, to non-Newtonian flow in polymer solutions, capillary viscometers fall short, since the required dynamic measurements cannot be made in a capillary viscometer.

Chapter III

CAPILLARY VISCOMETERS AND CORRECTIONS TO POISEUILLE'S EQUATION

1. Introduction. A variable shear viscometer is essentially an absolute instrument, since one is interested in determining the viscosity as one varies the driving pressure. One therefore has to ascertain whether the geometrical head does indeed represent the effective hydrostatic head, whether the volume of the liquid discharged in flow corresponds to the volume found by an independent calibration, etc. Ordinarily, one is not so concerned with these questions since these effects are supposed to be all lumped together in an apparatus constant, which will cancel, if one is only interested in relative measurements when the kinetic energy correction has been made negligible by suitable design. From a consideration of Poiseuille's equation in its usual form

$$\eta = \frac{\pi R^4 hgd}{8VL} \cdot t - \frac{mV}{8\pi L} \frac{1}{t} \qquad \text{(III - 1)}$$

it is clear that we are concerned with the radius of the capillary, R, the effective hydrostatic head, h, the effective driving pressure, hgd, the volume, V, and the length of the capillary.

The radius of the capillary should be uniform throughout its length. This requirement is easily met by the use of precision bore tubing. The radius should not be too small, otherwise dust particles will too readily lodge in the capillary and absorption may significantly diminish the radius.

The effective hydrostatic head requires careful consideration. Poiseuille's equation is derived for measurements at constant pressure. In ordinary viscometers the head changes continuously during a measurement as the meniscus is falling in the efflux bulb. We have to derive therefore an expression for the time average head.

The effective driving pressure will be equal to the product $h_{eff.}gd$ if the hydrostatic head is not too small. If however, the value of this product is such that the potential energy available for flow is of the same order of magnitude as the energy of the liquid surface on the inside of the efflux bulb, serious difficulties arise. To fix ideas about the orders of magnitude involved, we will consider a bulb with a volume of 0.20 ml and an inner surface of approximately 2 cm^2. Let the effective hydrostatic head be 2 cm of water. The potential energy for flow, then, amounts to 0.2 cm^3 x 981 dyne/gm x 1gm/cm^3 x 2 cm = 400 dyne cm. The energy of the liquid layer adhering to the wall of the bulb will be, in the case of an aqueous solution, 2 cm^2 x 72 dyne/cm = 144 dyne cm. Since this energy will not be available for flow, neglect of

this effect introduces a considerable error. It is also clear, that at ordinary hydrostatic heads, which are of the order of 10 to 20 cm, this correction becomes quite unimportant, particularly as the volume of the bulb is, for other reasons, larger when the head is larger. In the viscometry of Newtonian liquids this correction has only been considered in the very accurate work of Swindells (65), on the determination of the absolute viscosity of water, at the National Bureau of Standards.

The actual volume of the bulb can easily be found by a suitable calibration, but this volume is not necessarily equal to the volume in flow. As is well known, a certain amount of liquid is left behind after "complete" discharge. It can be shown that this amount is independent of the liquid, if, but only if, the liquid falls under its own weight. If the liquid is discharged under external pressure, either positive or negative, a drainage correction must be applied.

In practice, the length of the capillary appears to be slightly larger than the measured length. This is attributed to the inertia of the liquid. On leaving the capillary the liquid flows on for a while as if it were still in the capillary.

We shall now discuss quantitatively the corrections that must be considered in applying Poiseuille's equation to data obtained in a capillary viscometer.

2. Absorption Effects in the Capillary. Ohrn (39) has focussed the attention on a possible explanation of the anomalous values of the reduced specific viscosity observed with polymer solutions at very low polymer concentrations. Absorption of polymer molecules at the capillary wall would have two effects

a) decreasing the concentration of polymer in solution, and hence decreasing the flow time

b) decreasing the capillary radius, and hence increasing the flow time.

Considering only the influence of a smaller radius, Ohrn derives the expression

$$\left(\eta_{sp}/c\right)^* = \eta_{sp}/c + \frac{\eta_r}{c}\,\frac{4a}{R} \qquad \text{(III - 2)}$$

where: $\left(\eta_{sp}/c\right)^*$: apparent reduced specific viscosity

η_{sp}/c : actual reduced specific viscosity

a: thickness of the absorbed layer

When the thickness of the absorbed layer is much smaller than the radius of the capillary ($a \ll R$) the second term may still be appreciable at small concentrations. Equation (III - 2) is borne out by experiment. The effect is not significant at the concentrations at which measurements are usually made in studying the viscosity of dilute polymer solutions, provided that the radius of the capillary is 0.025 or greater. This

radius then represents the lower limit for any viscometer designed for dilute solution measurement. A capillary of this (or greater) radius has another advantage, it is not likely to be obstructed by occasional dust particles.

3. The Effective Hydrostatic Head. It has been pointed out (2) that the "effective" head in flow is not necessarily equal to the algebraic average of the initial and final heads, or the "time average" head (that is the head at the moment when flow has proceeded for half the ultimate flow time). An exact analysis reveals that the effective head depends upon the shape of the bulb.

For the cylindrical bulbs Barr (2) derives the following relation

$$h = \frac{h_i - h_f}{\ln {}^{h_i}/_{h_f}} \qquad \text{(III - 3)}$$

h_i: initial head

h_f: final head.

For spherical bulbs, the average mean head is calculated in the following way.

The volume of a spherical segment of height b for a sphere with radius R, is

$$V = \frac{1}{3}\pi b^2(3R - b) \qquad \text{(III - 4)}$$

Differentiating this expression with respect to b gives

$$dV = (2\pi Rb - \pi b^2)db \qquad \text{(III - 5)}$$

If the kinetic energy correction is negligible, we have from Poiseuille's equation

$$dV = \frac{\pi R^4 P}{8 \eta L} dt \qquad \text{(III - 6)}$$

Equating (III - 5) and (III - 6) gives the differential equation

$$(2\pi Rb - \pi b^2)db = \frac{\pi R^4 P}{8 \eta L} dt \qquad \text{(III - 7)}$$

We now express the hydrostatic head in terms of the geometry of the bulb. After half the volume is discharged, we have $h = h_o$

hence at $t = 0$ $h = h_o + R$ and $P = P_o = gd(h_o + R)$

at $t = \theta$ $P = P_o - gdb$.

Substitution of this in (III - 7), gives

$$(2\pi Rb - \pi b^2)db = \frac{\pi R^4}{8\eta L}(P_o - dgb) = \frac{\pi R^4 dg}{8 \eta L}\left[(h_o + R) - b\right] \qquad \text{(III - 8)}$$

Or, after rearrangement

$$d\theta = \frac{2\pi R}{A} \frac{b}{(h_o + R) - b} db - \frac{\pi}{A} \frac{b^2}{(h_o + R) - b} db \qquad \text{(III - 9)}$$

where: $A = \frac{\pi R^4 dg}{8\eta L}$

When this is integrated between the limits $\theta : 0 \rightarrow t$ and $b : 0 \rightarrow 2R$ the result can be expressed as

$$h = \frac{4/3\ R}{2c - (c^2 - 1)\ln \frac{c + 1}{c - 1}} \qquad \text{(III - 10)} \qquad c = \frac{h_o}{R}$$

This is the expression for the effective hydrostatic head, for flow out of a spherical bulb (2).

Since in this derivation, dV, obtained from the geometry of the bulb, was equated with dV, obtained from an expression describing the flow, which is only valid for non-Newtonian liquids, the relationship obtained will not be valid for non-Newtonian liquids.

Tuynman (6,) has taken into consideration non-Newtonian behaviour and derived expressions for viscometers with cylindrical bulbs.

For the case of relatively large shear gradients, for which the viscosity depends linearly on the shear rate

$$q = \frac{pR}{2L}\frac{1}{\eta}\left(1 + \alpha\frac{pR}{2L}\right)$$

Tuynman obtained the expression

$$t = \frac{8\eta LV}{\pi R^4 d}\frac{1}{\Delta h}\ln\frac{P_o}{P_1} - \frac{R^3 d\,\alpha}{2_o\eta^2 L^2(\Delta h)^2}\left[\frac{8\eta LV}{\pi R^4 d}\right]^2 (P_o - P_1) \qquad \text{(III - 11)}$$

where: P_o: P at t = 0

P_1: P at t = t

Δh: $h_i - h_f$

The second term represents the influence of non-Newtonian behaviour.

For the case of low shear gradients, for which the viscosity has a quadratic dependence on the shear rate

$$q = \frac{PR}{2L}\frac{1}{\eta}\left[1 + \beta\left(\frac{PR}{2L}\right)^2\right]$$

he obtained the expression

$$t = \frac{8\eta LV}{\pi R^4 d}\frac{1}{\Delta h}\ln\frac{P_o}{P_1} - \frac{\rho R^3 d}{20\eta^2 L^2}\frac{1}{t}(P_o^2 - P_1^2)\left(\frac{8\eta LV}{\pi R^4}\right)^2 \quad \text{(III - 12)}$$

Here too, the second term represents the influence of non-Newtonian behaviour. Tuynman's expressions apply only to viscometers with cylindrical bulbs. I have derived the analogous expressions for viscometers with spherical bulbs, by the method outlined above.

For large shear rates the expression is

$$t = \frac{\pi(h_o^2 - R'^2)}{A}\ln\frac{A(h_o - R') + B(h_o^2 - R'^2)}{A(h_o + R') + B(h_o^2 - R'^2)} + \frac{2\pi R' h_o}{A + Bh_o} \quad \text{(III - 13)}$$

where: $A = \dfrac{\pi R^4 dg}{8L\eta}$

$$B = \alpha\frac{\pi R^5 e^2 g^2}{20\eta^2 L^2}$$

R' = radius of spherical bulbs

For low shear rates, the expression is

$$t = \frac{\pi}{2A}(h_o^2 - R'^2)\ln\frac{A(h_o + R')^2 + C(h_o^2 - R'^2)^2}{A(h_o - R')^2 + C(h_o^2 - R'^2)^2} + \frac{4\pi R' h_o}{A} - \frac{2\pi h_o R}{A + (h_o^2 + R^2)C} \quad \text{(III - 14)}$$

where: $C = \beta\dfrac{\pi R^6 e^3 g^3}{48\eta L^3}h^3$

The expression for a Newtonian liquid is obtained by setting

$B = C = 0$

$$t = \frac{\pi}{A}(h_o^2 - R'^2) \ln \frac{h_o - R}{h_o + R} + \frac{2\pi h_o R'}{A} \qquad \text{(III - 15)}$$

This can be shown to be equivalent to (III - 10).

As is evident the expressions are rather cumbersome, but they are given for the sake of completeness. The relative importance of the non-Newtonian terms cannot be readily indicated, since reliable values of a and b could not be found. When those values are obtained, it would be rather interesting to calculate the non-Newtonian terms. In this thesis the effect of the non-Newtonian behaviour on the effective hydrostatic head is ignored, mainly because of other corrections, that are certainly orders of magnitude larger.

4. Surface Tension Correction. This correction has received relatively little attention, even though it is the major correction at low hydrostatic heads. There are two points of view on how to calculate this correction. If the effect could be quantitatively accounted for by the liquid layer adhering to the inner surface of the efflux bulb, it would be relatively easy to eliminate it--at least in an Ostwald viscometer--by making the upper and lower bulb of exactly the same shape and size. Sprokel (62) designed a series of Standard Ostwald viscometers, for which the surface tension correction was taken care of in this way. He showed that, taking also into account the so-called "filling-error" (an error that applies only when

Ostwald and Ostwald-type viscometers are not filled with a volumetric pipet) the surface tension effect was eliminated if the following expression is valid

$$\frac{A_1 - A_2}{V} + \frac{2\, r_{cap}}{r_2^2}\left[1 - \frac{r_{cap}}{r_b}\right] = 0 \qquad \text{(III - 16)}$$

where: A_1: area of upper bulb

A_2: area of lower bulb

r_{cap}: radius of capillary

r_2: radius of cylindrical lower bulb

r_b: radius of limb extending from lower bulb

The first term takes account of the differences in inner surface of the upper and lower bulb, the second term arises from the filling error.

His calibration with water, sucrose solutions and organic solvents confirmed the absence of a surface tension effect in his viscometers. It should be pointed out, however, that the average hydrostatic head in his viscometer was 12 cm.

The other point of view is that of Barr (3). He calculates the mean capillary rise in the bulb and subtracts this from the average calculated head. The mean capillary rise is evaluated as

$$\langle h_\gamma \rangle = \frac{\sum \Delta V_i\, h_{\gamma i}}{\sum_i \Delta V_i} \qquad \text{(III - 17)} \qquad \sum_i \Delta V_i = V$$

The required h_γ can be calculated for any form of vessel, with

the aid of the Tables calculated by Bashforth and Adams [4]. Swindells [65] used the same method to take account of the surface tension effect in Bingham viscometers used in the determination of the absolute viscosity of water, and found excellent agreement between the so calculated correction and the experimentally observed one. Therefore we have followed Barr's procedure to correct for the surface tension effect.

The method is as follows.

In order to be able to calculate the capillary rise, one has to know the radius of curvature of the meniscus. The contour of the meniscus is characterised by the parameter

$$\beta = b^2 \frac{dg}{\gamma} \qquad \text{(III - 18)}$$

b: radius of curvature at the vertex O

γ: surface tension

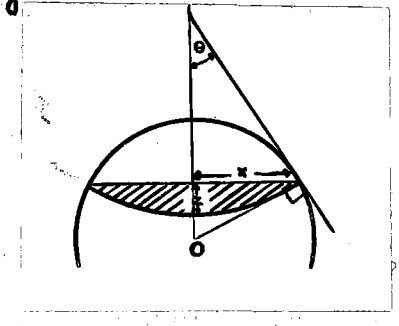

In the tables of Bashforth and Adams the ratio's x/b and z/b are given for values of β ranging from 0.125 to 100. If the surface tension and density are known for a liquid, each value of b determines a value of β, and hence a series of values of x and z. These values are listed for stated values of the angle ϕ between the vertical through the axis of revolution of the meniscus and the normal to the bounding

surface (the values of ϕ covering the range 0° to 180° in five degree intervals). For cylindrical bulbs this angle is 90°, for spherical bulbs the angle varies from 0° to 180°.

The calculation for spherical bulbs was made as follows:

For all tabulated values of β, b and b^2 were calculated for benzene and water at 20° C. For a given size of bulb x was calculated for values of ϕ ranging from 165° to 15°. These values were designated as $x_{required}$.

Since we had already calculated all the b values for all the β's listed, x/b was looked up for a certain angle ϕ. This was multiplied by the known b, and the x-value so obtained compared with the required x-value. By trial and error these two x-values were brought as close as possible into agreement with each other. By linear interpolation a further approximation was obtained. In this way the actual value of x/b was obtained for fractional values of β. As an internal check this x/b value was multiplied by a b value obtained from our tables, using the same interpolation factor. The value of x so obtained was compared to $x_{required}$. In all cases excellent agreement between these values was obtained. Having determined b, the capillary rise was calculated as

$$h_\gamma = \frac{2\gamma}{dg}\frac{1}{b} \qquad \text{(III - 19)}$$

The next problem is to calculate the amount of liquid discharged between two successive values of x, taking into account both the volume of the "drop" and the geometrical volume. The volume of the shaded portion of fig. can also be calculated from Bashforth and Adams Tables, inasmuch as it actually represents a drop upside down.

The values listed in the tables are the values of V/b^3, corresponding to a given value of β. The geometrical volume was calculated as the difference between the volumes of the spherical segments with two successive x-values as base. The required ΔV can then be calculated as

$$\Delta V = \Delta V \text{ geom} - V_\beta (x_k) + V_\beta (x_\ell) \qquad \text{(III - 20)}$$

where: $\Delta V \text{ geom} = V^{x_\ell}_{\text{geom}} - V^{x_k}_{\text{geom}}$

$V_\beta(x_k)$: volume of "drop", with x_k as base.

This value of ΔV was multiplied by h_γ, and the mean capillary rise was calculated according to (III - 17).

5. The Kinetic Energy Correction. This correction, already calculated in the preceding Chapter, is expressed by a term

$$- m \frac{V}{8\pi L} \cdot \frac{1}{t}$$

in the modified Poiseuille equation. The constant m has to be determined by calibration. It is of the order of unity, but it may vary by more than 100% from one viscometer to another. Moreover it is a function of the velocity of flow,

as was first observed by Swindells (65) in the calibration of Bingham viscometers. This makes the quantitative aspect of the kinetic energy correction rather uncertain. The safest thing to do is to design the viscometer so that $V \ll Lt$ and hence the correction is negligible.

When, however, the correction must be applied--as it must at high external pressures--it is well to know how it is affected by non-Newtonian flow. For convenience we will write the Poiseuille equation, corrected for kinetic energy as

$$\eta = \frac{\pi R^4 t}{8VL}\left[P - md\left(\frac{V}{\pi R^2}\frac{1}{t}\right)^2\right] \qquad \text{(III - 21)}$$

where the quantity in brackets denotes the effective driving pressure. We will now give the derivation, due to Hermans and de Wind (17), of an expression by which the kinetic energy correction can be evaluated.

For high shear gradients it may be assumed that the viscosity depends linearly on the shear rate or shear stress.

$$\eta^* = \eta - a_1 q \qquad \text{(III - 22)} \qquad \eta^*: \text{apparent viscosity}$$

This assumption enables us to calculate Q, as

$$Q = 2n\int_0^R vrdr = \frac{\pi L^3}{P^3}\int_0^{PR/L} \tau^2 F(\tau)d\tau \qquad \tau = \frac{PR}{L} = 2\eta^* q$$

Carrying out the integration, one obtains

$$\frac{1}{t} = \frac{p}{B}\left[1 + \frac{2}{5}a_1 \frac{Rp}{\eta^2 L}\right] \qquad \text{(III - 23)} \qquad B = \frac{8\eta LV}{\pi R^4}$$

This can be regarded as a quadratic equation in p ; solved for p , it leads to

$$p = \frac{B}{t} - \frac{2}{5}a_1 \frac{RB^2}{\eta^2 L}\frac{1}{t^2} \qquad \text{(III - 24)}$$

In order to take the kinetic energy into account, we replace p by the effective driving pressure from (III - 21). This leads to the expression

$$p = \frac{B}{t} - \frac{C_1 - C_2}{t^2} \qquad \text{(III - 25)} \qquad C_1 = \frac{mdV^2}{\pi^2 R^4}$$

$$C_2 = \frac{128}{5}\frac{V^2 L}{\pi^2 R^7}a_1$$

Or $$pt = B + \frac{C}{t} \qquad \text{(III - 26)} \qquad C = C_1 - C_2$$

The interesting result of this calculation is that, to a first approximation a Newtonian liquid gives rise to linear pt vs $1/t$ plots. In order to separate the two contributions to the slope of the pt vs $1/t$ plot one proceeds as follows.

For the solvent $a_1 = 0$, hence $C_2 = 0$ and C_1 can be calculated as the slope of a pt vs $1/t$ plot.

For a non-Newtonian liquid the slope C is determined and C_2 obtained as $(C_1 - C)$.

At low gradients (III - 22) is known not to hold and has to be replaced by

$$\eta^* = \eta - a_2 q^2$$

Proceeding as before, one obtains

$$\frac{1}{t} = \frac{p}{B}\left[1 + \frac{a^2}{6}\frac{R^2p^2}{\eta^3L^2}\right] \qquad \text{(III - 27)}$$

and

$$p = \frac{B}{t} - \frac{a^2}{6}\frac{B^3R^2}{\eta^3L^2}\frac{1}{t^3} \qquad \text{(III - 28)}$$

Taking into account the kinetic energy correction (III - 28) becomes

$$p = \frac{B}{t} + \frac{C_1}{t^2} - \frac{D}{t^3} \qquad D = \frac{a^2}{6}\frac{B^3R^2}{\eta^3L^2}$$

Or

$$pt = B + \frac{C_1}{t} - \frac{D}{t^2} \qquad \text{(III - 29)}$$

(if even (III - 29) fails to represent the data, a different method can be applied. For this method, however, the original paper should be consulted (1)).

Equation (III - 29) is seldom needed, since at low shear stresses the kinetic energy correction will be negligible.

If high shear stresses are achieved with the aid of external pressure, equation (III - 26) should be used with caution, since the drainage effect also makes a contribution to the slope of a pt vs 1/t plot.

6. <u>The Drainage Correction</u>. An exact analysis of the drainage phenomenon in cylindrical tubes has been made by Tuynman (69).

He derives for the volume of liquid left behind after a time t

$$\Delta V = \frac{4}{3}\pi r t v \left(\frac{\eta v}{gd}\right)^{1/2} \qquad \text{(III - 30)}$$

$v = Q/\pi r^2$

r : radius of the tube

For a given tube t v is constant, hence

$$\Delta V = \frac{4V}{3}\left(\frac{\eta v}{gd}\right)^{1/2} \qquad \text{(III - 31)}$$

From this result it follows that, for free fall, V becomes independent of both the viscosity and the density, and is equal to

$$\Delta V = \frac{4}{3} V \frac{R^2}{r}\left(\frac{\pi h}{8L}\right)^{1/2} \qquad \text{(III - 32)}$$

R: radius of the capillary

An important consequence of this is that in measurements of relative flow times t_r -- and therefore η_r, η_{sp} and $[\eta]$ -- no drainage correction need be applied so long as the measurements are made at free fall.

If, however, external pressure is applied, v becomes porportional to p/η , hence

$$\Delta V = k\sqrt{\frac{P}{d}} \qquad \text{(III - 33)} \qquad k = \frac{4VR^2}{3r^2}\sqrt{8Lg}$$

If we may neglect the kinetic energy correction for the time being, we have

$$Q = \frac{V - \Delta V}{t} = \frac{V - k(P/d)^{1/2}}{t} = \frac{\pi R^4 p}{8\eta L}$$

Or

$$pt + \frac{8kL}{\pi R^4}\left(\frac{\eta}{\sqrt{a}}\right)\sqrt{p} = \frac{8\eta LV}{\pi R^4} \qquad \text{(III - 34)}$$

Hence a plot of pt vs $p^{1/2}$ should give a straight line, with a slope proportional to $\eta/d^{1/2}$ and an intercept proportional to η.

A more empirical treatment is due to Fuoss and Cathers (24). They consider that V, the volume retained on the walls of the viscometer bulb, should depend on the density, viscosity and flow time in the following way

$$V = \rho \frac{V\eta}{dt} \qquad \text{(III - 35)}$$

The actual working volume, then, is equal to

$$V = V_o \left[1 - \frac{\rho\eta}{dt}\right] \qquad \text{(III - 36)} \qquad V_o: \text{dry volume of the bulb}$$

Substituted in Poiseuille's equation, this leads to

$$pt = \frac{8\eta L V_o}{\pi R^4} \left[1 - \frac{\rho\eta}{dt}\right] \qquad \text{(III - 37)}$$

The drainage correction can in this way be evaluated from a pt vs 1/t plot.

The influence of non-Newtonian behaviour of the liquid on the drainage correction cannot be calculated rigorously. An attempt was made to derive the drainage correction for spherical bulbs, but difficulties were encountered in regard to the assumptions that one has to make for a liquid draining from a curved surface. It was therefore decided to treat drainage in the manner proposed by Fuoss and Cathers.

7. The End-Correction. As already stated, this effect is due to the inertia of the liquid, when flowing out of an orifice. Because the liquid tends to flow in the same manner as in the capillary for a short distance outside the capillary, the capillary appears to be longer than actually measured. The correction takes the form of

$$L_{eff} = L_{meas} + nR \qquad (III - 38)$$

R: radius of the capillary

n: constant equal to 1.64

This correction is significant only for short capillaries. With capillaries 30-50 cm long--as in our viscometers (Chapter V)--this correction can be safely ignored.

8. Discussion. It is clear from what has been said in Section 1 and 2 that absorption and the calculation of the effective hydrostatic head do not present any difficulties. Absorption effects are eliminated by choosing radii larger than 0.025 cm. The hydrostatic head can be calculated. In section 3 we have shown how the mean capillary rise can be calculated, but this calculation is rather involved and time consuming, hence one should eliminate this correction. It was shown, how one could eliminate this correction for an Ostwald viscometer. Since, however, polymer chemists are not so much interested in the value of the viscosity of a solution as in the dependence of the viscosity of a solution on the concentration of the solute,

it is convenient to be able to alter the concentration by making dilutions in the viscometer itself. This is not practicable in an Ostwald viscometer. In fact, the only type of viscometer in which this is practicable is a suspended-level Ubbelohde viscometer. In his original papers Ubbelohde showed that the surface tension effect can be eliminated by means of a curved suspended level, whose radius of curvature is such, that the pressure exerted by this curved surface exactly balances the decrease in head due to the mean capillary rise in the efflux bulb. He further claimed that the same curved surface eliminated surface tension effects for all liquids.

Data obtained with the viscometers described in this thesis clearly show that this is not the case at low driving pressures. This observation led us to design two different series of viscometers, Series II for use with organic solvents and solution in these, and Series III for use with water and aqueous solutions. The required radius of curvature was calculated from the expression

$$R_o = \frac{2\gamma}{dg} \frac{1}{\langle h_\gamma \rangle} \qquad \text{(III - 39)}$$

The calibration data show that the surface tension effect is indeed eliminated in the series II viscometers (II-A and II-B), and, for water in the series III viscometer.

In Sections 3 and 4 we have derived expressions for the drainage and the kinetic energy corrections. Unfortunately not only drainage effects but kinetic energy and non-Newtonian effects as well can contribute to the slope of the suggested pt vs 1/t plot.

For high shear stresses, the combined equation runs

$$pt = \frac{8\,LV}{R^4} + \frac{mdV^2}{2_R 4} - \frac{8\,LV}{R^4}\,\frac{1}{d} - \frac{128}{5}\,\frac{V^2 L}{2_R 7}\,a_1\,\frac{1}{t} \qquad \text{(III - 40)}$$

If a calibration is carried out with a Newtonian liquid of about the same viscosity as the non-Newtonian liquid to be studied, then the first two terms can be evaluated. The slope so obtained can be compared with the slope obtained for the non-Newtonian liquid, the difference being the influence of the non-Newtonian term.

For low shear stresses, the drainage effect need not be considered, provided one uses viscometers with a number of bulbs furnishing a range of heads, for all the measurements could then be made at free fall and hence no drainage correction would be necessary. Moreover the kinetic energy correction could be designed out by a suitable choice of the volumes of the bulbs.

Chapter IV

THE SIGNIFICANCE OF THE MEASUREMENT OF NON-NEWTONIAN FLOW IN CAPILLARY VISCOMETERS

In this chapter we will deal with the experimental observations of non-Newtonian flow and discuss their significance in terms of recent theories. We will discuss first the experimental evidence and then the experimental technique.

1. Experimental Investigations of non-Newtonian Flow.

"Anomalous" flow behaviour of colloidal solutions was first observed in the early twenties by Wolfgang Ostwald ([42]). Staudinger ([63]), in his researches on high-molecular weight compounds, noted similar "anomalies". Since this flow behaviour was attributed to the build-up or breakdown of a structure in the liquid, Ostwald proposed for it the name "structural viscosity" (Strukturviskosität). Staudinger saw in the occurrence of structural viscosity additional evidence for his contention that the compounds he was studying were high-molecular weight compounds rather than association colloids: at higher temperatures the structural viscosity persisted, as one would expect if the solute particles were single giant molecules, but as one would not expect if they were colloidal aggregates. An excellent summary of the earlier work can be

found in Staudinger's book Hochmolekulare Organische Verbinduqen (1932). Non-Newtonian behaviour was observed with all types of macromolecular compounds, whether natural or synthetic, provided that the molecular weight was sufficiently high.

Philippoff (45) made a thorough study of non-Newtonian flow giving considerable attention to the problem of describing it adequately. He and Reiner (49) suggested that data be presented in the form of plots of log τ vs log q. The general features of such a plot--which they called a "flow-curve"--for a non-Newtonian liquid are as follows: At low stresses the slope is unity and hence the liquid is Newtonian; at intermediate stresses the slope is greater than unity (which means the liquid is non-Newtonian) and the curve passes through a point of inflection; at high stresses the slope is unity and the liquid is again Newtonian.

This general shape could be accounted for in terms of random orientation of the molecules at low stresses, increasing orientation in the direction of flow at intermediate stresses, and complete orientation at high stresses. Additional evidence for this orientation theory was found by Staudinger (63) in Signer's work on flowbirefringence (59).

The flow curve representation of non-Newtonian flow offers three parameters for the characterization of a non-Newtonian system. Both at high and low stresses the liquid is

Newtonian, and hence two viscosities can be clearly defined. The third parameter is the point of inflection which occurs at some definite shear stress. A correlation of these reference points with the structural parameters of the molecule could not be made, however, since no polymer samples characterised by independent measurements were available. Moreover, a general theory of solution behaviour of the macromolecule did not exist. Only recently has sufficient theoretical information accumulated to guide experiments and provide clues to the meaning of the experimental observations.

We will now discuss what information can, in principle, be obtained, and to what extent the obtaining of this information is possible with capillary viscometers.

It must be realised that the theories dealing with non-Newtonian flow in dilute polymer solutions are strictly applicable only to solutions so dilute that the molecules may be regarded as isolated entities in solution that do not interact with each other. This means that the concentration should be well below the so-called "critical concentration", i.e. the concentration at which the molecules just touch each other. A convenient way of calculating this concentration is given by Bigelow (6), who found the expression

$$C_{crit} = \frac{0.0436}{[\eta]} \qquad (IV - 1)$$

to hold in a wide variety of systems. For non-Newtonian

systems the intrinsic viscosity, $[\eta]$, should be replaced by the intrinsic viscosity at zero shear stress, $[\eta]_{I=0}$. For a typical shear dependent solution of polystyrene (intrinsic viscosity, 10 dl/gm) this would mean that viscosity determinations should be made at concentrations lower than 0.00436 gms/100 ml. Measurements at such low concentrations are difficult to make with sufficient precision: the quantity to be determined is $\eta_r - 1 / c$ and at very low concentrations both η_r and c are small and small errors in these lead to large errors in their ratio. Moreover the slightest amount of absorption would affect the concentration, and hence the flow times, very much. We will discuss the effect of shear stress on the intrinsic viscosity only, not on either the relative viscosity or the reduced specific viscosity, since, to a first approximation at least, the effect of interaction is eliminated by extrapolation to zero concentration of data obtained at finite concentrations, usually well above the critical concentration. There is another reason to limit consideration to the intrinsic viscosity. Since the dependence of the viscosity of a solution on the concentration is not understood in sufficient detail ([23]), because of the difficulty of calculating the hydrodynamic interaction between molecules, it would be hazardous to try and interpret the influence of shear stress on a concentration-dependent variable such as η_r or $\eta_r - 1 / c$.

For rigid molecules (cellulose and polyelectrolytes, for example) the theory has been worked out in sufficient detail to allow a quantitative evaluation of the structural parameters. Peterlin (44), derives for the dependence of the intrinsic viscosity on the shear stress

$$[\eta]_q = [\eta]_0 \left(1 - \left[\frac{R^2/qD^2}{8\eta_0^2}\right]\tau^2 \cdot \cdots \right) \qquad (IV - 2)$$

where: R: root mean square end-to-end distance

D: rotational diffusion coefficient

Since the rotational diffusion constant also depends on the size of the molecule and hence on the root-mean-square end-to-end distance, the coefficient of τ^2 depends only on the size of the molecule. This dependence has been calculated by Scheraga (51). Comparison of the experimentally observed shear dependence and the theoretically predicted one, leads to a complete evaluation of size and shape of the solute. The most striking illustration of this can be found in the work of Eisenberg (19) on DNA. He determined the size and shape of the DNA-molecule from an exact analysis of the shear dependence and from measurements of light-scattering and sedimentation, and obtained by the two methods values that were in excellent agreement. A study of the shear dependence is especially rewarding with polyelectrolytes (at low ionic strength, when the molecules are rigid) since reliable light-scattering data can be obtained only with difficulty, because

of the impossibility of obtaining optically clean solvent. For rigid molecules at least, the theory is able to account quantitatively for the observed effects.

The theory for flexible molecules is not as conclusive as the one for rigid molecules. Besides orientation, one has to consider deformation of the molecule. There are two factors opposing this deformation, one being the inner viscosity ( ) of the molecule, presumably resulting from the restricted rotation about the valence bonds, the other the increased asymetric hydrodynamic interaction in the deformed state(13) A consideration of either one of these factors can lead to a reasonable description of the shear dependence of the intrinsic viscosity of a flexible molecule. Cerf(9) has indicated how one could determine the relative influence of these effects, if the shear dependence is studied in solvents of different viscosity. The inner viscosity depends on the viscosity of the solvent; the hydrodynamic interaction does not, at least to a first approximation, since it is merely due to a change in shape of the molecule. If this picture is correct, then it would lead to an interesting way of detecting differences between branched and linear molecules. It can be shown (64), that a branched molecule has a higher segment density than a linear molecule of the same size. If the intersegmental hydrodynamic interaction is only changed by a change in shape, then one would expect the

branched molecule to have a higher internal viscosity than a linear one. Investigations of the type indicated above have not been conducted systematically, and the information is rather scanty. It would, however, be perfectly feasible to obtain the necessary data with a reliable capillary shear viscometer.

2. Measurement of Non-Newtonian Flow in Capillary Viscometers.

The quantity of greatest interest to polymer chemists is the intrinsic viscosity at zero shear stress, for this is the quantity that provides a measure of the volume of the molecule when undistorted by shear effects. This quantity obviously cannot be measured directly, but it is obtainable by extrapolation from measurements at low finite shear stresses. In order that the extrapolation may be reliable the measurements should be made to as low a shear stress as possible. We will now discuss how and to what extent this can be done in capillary viscometers.

The shear stress at the wall of a capillary tube is given by

$$\tau_R = \frac{hgd\,R}{2L}$$

Hence a lower shear stress is favoured by (a) a smaller radius of the capillary, (b) a greater length of capillary tubing, and (c) a smaller hydrostatic head.

The radius of the capillary should not be smaller than

0.025 cm if difficulties due to absorption and dust particles are to be avoided (Chapter III).

The length of the capillary can be as large as desired, and it should be long, to make the kinetic energy correction ($mV/8\pi Lt$) small. There are two limiting factors, however; the viscometer must be of manageable dimensions (not too long to fit in a bath in which a good uniform temperature can be achieved), and the hydrostatic head must be small.

With a capillary of fixed radius and length, low hydrostatic heads can be obtained

(a) by using a horizontal capillary. The limiting head is determined by the capillary rise in the bulb system. A very long horizontal capillary makes the viscometer, however, very fragile.

(b) by tilting the viscometer. In this case the effective head is given by:

$$h_{eff} = h_o \cos\alpha \qquad \alpha: \text{angle of tilt}$$

the disadvantage of this method is that drainage effects may become rather large and uncalculable.

(c) By bending the capillary in a shallow helix. Here the liquid enters the helix from the bottom, flows upwards and at the top of the helix is taken down to the reservoir bulb, below the beginning of the helix. Bending the capillary has two disadvantages, if the viscometer is used

at other than low driving pressures an apparent increase in the viscosity will be observed, due to the fact that the liquid will tend to oscillate in the curved capillary (15,12). Moreover the uniformity of bore will certainly be partly destroyed in the actual process of bending.

(d) By dividing the capillary into two vertical sections. The liquid flows up in one section and down in the other. This method, which is by far the most preferable, has been generally overlooked, although it was used by Kruyt and coworkers (21) as early as 1927.

It is clear then, that low shear stresses can be obtained in capillary viscometers.

It is better to build a low hydrostatic head into the viscometer than to depend on external control of driving pressures, because of the difficulty of maintaining small pressures with a manostat. The practical limit of hydrostatic head is about 2 cm. This lower limit depends mainly on the capillary rise in the tubing connecting the bulbs. A common diameter for this tubing is 0.2 cm. For water the capillary rise is 1.46 cm, for benzene 0.66 cm. Since the meniscus should fall at a perceptible rate when it reaches the lowest mark, the practical limit is indeed about 2 cm. Thus with a capillary of a radius of 0.025 cm and a capillary length of 100 cm, a shear stress of 0.5 dynes/cm^2, or a shear rate of 50 sec^{-1}, can be obtained for a liquid with a viscosity of

one centipoise. These lower limits are adequate for not-too-shear-dependent systems.

The capillary viscometer would, therefore, appear to be a very suitable instrument for making measurements at low shear stresses. And it would be if it were not for the surface tension effect. As already indicated, the surface tension correction may amount to about 30% at these low driving pressures. Another effect has to be considered in Ostwald- or U-tube viscometers. In these viscometers, the liquid level falls in the one limb and rises in the other. Precision measurements (31) indicate that there is a small yield value associated with the advancing of the meniscus, due either to incomplete wetting or to a difference in surface tension between the advancing surface and the receding surface (60). This small yield value will change the shape of the viscosity vs. shear stress plot in such a way that an almost exponential dependence is observed instead of a quadratic dependence. Hence an extrapolation to zero shear stress will become very difficult in these viscometers. An effect of this nature is indicated in the work of Golub ( ).

3. Typical Variable Shear Viscometers.

Several different viscometers, and several modifications of the Ostwald-type viscometer, have been described and used in shear studies. Most of them have drawbacks more or less serious. We will discuss only the more significant of these

variable-shear viscometers, limiting ourselves to low-shear viscometers. High shear stresses can be obtained with almost any viscometer, if one has a suitable manostat to maintain constant high pressures and applies these externally. The results obtained should, however, be interpreted with caution, since wall-effects and the influence of local turbulence may be appreciable. With flexible molecules, one should not exclude the possibility of creating a concentration gradient across the capillary, induced by a free-energy gradient. Since the shear stress across the capillary varies from zero in the center of the tube to its maximum value at the wall, the molecule will be deformed to different degrees at different distances from the wall. Since deformation will decrease the entropy of the molecule, an entropy gradient will occur and hence a free energy gradient. This effect was noticed by Garner, Nissan and Wood (25).

4. Variable-shear Viscometers for Use at Low Shear Stresses.

(a) Modified Ostwald Viscometers. Modifications of the Ostwald viscometer have been proposed by Flory and Krigbaum (31) and Wada (72). The Flory viscometer has a horizontal capillary and only two measuring bulbs. No consideration was given to surface tension effects, but these would not have been of considerable influence since the viscometer was not capable of making measurements at very low shear stresses.

Wada's viscometer is designed for measurements at

extremely low shear stresses, which can be obtained by tilting the viscometer. Surface tension effects were considered and eliminated, but no details of the calculation have been published.

(b) U-tube viscometers ( ). In this type of viscometer the decrease of the hydrostatic head is determined as a function of time. As already pointed out, this viscometer must be considered inadequate for operation at extremely low shear stresses because of the hysteresis effects associated with an advancing and receding meniscus. Moreover, although non-Newtonian character of the flow is revealed by curvature in a plot of ln h vs t and the viscosity at a given shear stress can be calculated from the slope of a tangent drawn to this curve, the plot is such that it does not provide a sensitive indication of the shear dependence or yield precise values of the viscosity.

(c) Modified Ubbelohde Viscometers. The Ubbelohde viscometer is almost ideal for dilute solution work, since dilutions can be made in the instrument itself. Moreover, since it has a suspended level, there is no problem of an advancing meniscus. By a suitable choice of the radius of curvature of the suspended level, one can eliminate the need for a surface tension correction. The most widely used version is the one described by Schurz and Immergut (53). It has four closely spaced efflux bulbs and a rather short capillary, which makes

the instrument not very suitable for measurements at low shear stresses. The instrument has been much used in shear dependence studies with cellulose solutions.

Another modification is described by J. J. Hermans, Jr. (26). Here the capillary is wound in a helix, which, as we have already pointed out, is not too desirable. The important feature is, however, that the bulb system is replaced by a cylindrical tube of constant cross-section. This makes the various corrections much easier to calculate, but reduces the precision with which flow times can be measured. No indication in the original publication is given as to whether or not the suspended level was suitably modified to eliminate surface tension corrections.

(d) Bingham viscometers. This viscometer (7) was especially designed for use with external pressures, yet it has not been widely used in shear studies. The instrument is capable of high precision, and was used to determine the absolute viscosity of water. The disadvantage for low-shear studies is that one either has to make the instrument unduly long to incorporate a sufficient length of capillary or apply very small external pressures, which are difficult to maintain constant.

(e) Tilted capillary viscometer. In this viscometer the movement of a column of liquid is followed as it flows through an inclined capillary. Berneis (60) has explored the

possibilities of such an instrument. In principle the flow time should not depend on the length of the column of liquid, but because of surface tension effects it unfortunately does. Although Berneis was able to evaluate all the necessary corrections, one is left with the impression that the same information could be more easily obtained with other viscometers.

(f) Maron and Krieger Viscometer (38). In this viscometer the liquid is forced through a capillary by a falling column of mercury. Measurement of the column height as a function of time gives both the pressure drop and the flow rate. Lower driving pressures can be obtained with the aid of liquids less dense than mercury. This instrument does not function at very low shear stresses, but for shear measurements at intermediate and high stresses it is very good indeed.

This concludes the survey of the various low-shear viscometers proposed in the literature, but we should mention one other method, which does not involve the use of an especially designed viscometer, but enables one to determine the zero shear viscosity in a very elegant fashion. For any viscometer with a negligible kinetic energy correction one can derive for the relative flow time of a Newtonian and a non-Newtonian

$$1/t_r = \frac{\eta_s}{\eta_0}\left[1 + a_1 \frac{P^2R^2}{3\eta_0^2 L^2}\right]$$

Hence, if a series of measurements is performed on the same solution in viscometers of different capillary radii at the same pressure, the resulting plot of t_s/t_o vs R^2 will be a straight line. The intercept at $R^2 = 0$ gives the relative viscosity at $q = 0$. It must be pointed out that this treatment is only allowed if wall effects are absent; hence measurements should be made at as low driving pressures as possible.

5. Summary.

From these considerations it follows that the most satisfactory viscometer for shear measurements in the low shear range would be a modified Ubbelohde viscometer. It could be designed to eliminate kinetic energy and surface tension effects. It would permit dilution in the instrument. It could be made rugged and compact, even with a long capillary, by dividing the capillary as Kruyt did (21). The variable shear feature can be attained by incorporating several bulbs at different heights. At very low shear stresses a cylinder of constant cross section might be better but at intermediate shear stresses a bulb system is preferable, since, in order to obtain a sufficiently long flow time, the radius of the cylindrical tube would have to be so large that the rate at which the meniscus falls would be too small to be precisely measurable.

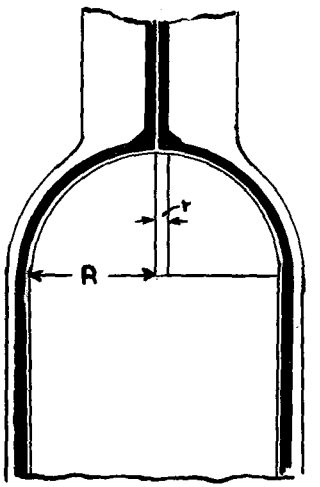

fig V

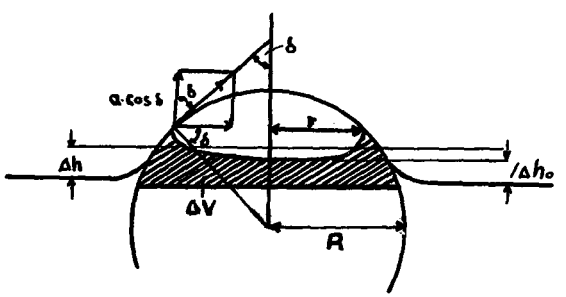

fig V-2

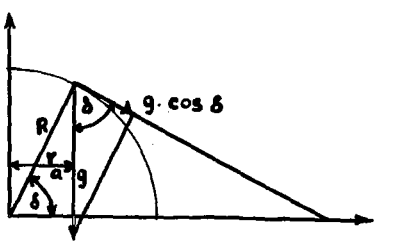

Fig V-1

Chapter V

THE DESIGN OF A VARIABLE-SHEAR UBBELOHDE VISCOMETER

1. Theory of the Suspended Level Viscometer [70].

The liquid flows first through a capillary, the volume discharged during a given time t being given by Poiseuille's equation, assuming a negligible kinetic energy correction, as

$$V = \frac{\pi g h R^4 t}{8 L \nu} \qquad (V - 1) \qquad \nu = \frac{\eta}{d} : \text{kinematic viscosity}$$

After leaving the capillary, the liquid flows over a curved hemispherical surface at a rate, calculable from the equation

$$V = t\, l^3 \frac{2\pi g}{3\nu} \frac{r_a^2}{R_o} \qquad (V - 2)$$

l : thickness of the suspended level

R_o : radius of curvature of the hemisphere

r_a : see fig. (V - 1)

Ubbelohde derived this equation for laminar flow with a free surface in a sloping channel, on consideration of Newton's hypothesis.

Equating (V - 1) and (V - 2) gives an expression for the thickness of the layer

$$l = \sqrt[3]{h} \cdot C \qquad (V - 3) \qquad C = \left[\frac{2}{16} \frac{R_o}{L} \frac{R^4}{r_a^2}\right]^{1/3}$$

It is seen that the thickness is independent of the kinematic

viscosity and only slightly dependent on the effective hydrostatic head h. This is rather fortunate since now the position of the suspended level will be the same for all liquids and will change only little if the hydrostatic head is altered. This means that the suspended level feature can be embodied in a variable shear viscometer.

Ubbelohde then deals with the surface tension correction. His treatment is, however, incorrect. His surface tension correction is calculated on the basis of the extra amount of liquid drawn up at the walls of the vessel, and supported by the surface tension (this extra amount being that which is above the horizontal plane tangent to the lowest part of the curved meniscus). The liquid is drawn up in a direction of the tangent to the curved surface where it joins the wall. The vertical component of the supporting force is therefore $2\pi r \gamma \cos\delta$. (See fig.٧-٢) The amount of liquid supported by the surface tension may then be calculated from the relation

$$2\pi r \gamma \cos\delta = \pi r^2 \Delta h\, d$$

It is seen from fig. V - 2, that $\cos\delta = r/R$, hence we obtain for Δh, which is the mean capillary rise of the bulb

$$\Delta h = 2\gamma / d R' \qquad (V - 4)$$

which means that one may treat a sphere as though it was a

cylinder, since the capillary rise in a cylinder of radius R is exactly the same as (V - 4). This is clearly incorrect. Moreover one is not interested in the capillary rise of the bulb, but in the "volume average"

$$\langle \Delta h_\gamma \rangle_v = \frac{\sum h_i \Delta V_i}{\sum \Delta V_i} \qquad (V - 5)$$

Hence the surface tension was calculated in a manner already described in Chapter III.

A correction must also be made for the capillary rise in the connecting tubing. The total correction for capillary rise between the two fiducial marks is given by

$$\langle h_\gamma \rangle = \frac{h_\gamma^{tube} \Delta V_1 + \sum h_i \Delta V_i}{\Delta V_1 + \sum \Delta V_i} \qquad (V - 6)$$

where: ΔV_1 : volume of connecting tubing
$\sum \Delta V_i$: volume of sphere

The required radius of the hemisphere is calculated as

$$R_o = \frac{2\gamma}{d} \frac{1}{\langle h_\gamma \rangle} \qquad (V - 7)$$

it being the pressure exerted by a curved surface of radius R_o. It follows from Equation (V - 7) that R_o depends on the surface tension and that, therefore, one should have different viscometers for liquids of different surface tension. Ubbelohde made the claim--based on his treatment of the surface tension correction--that one value of the radius of curvature would accommodate all liquids. This is probably true for the usual

Ubbelohde viscometer, which has a relatively large hydrostatic head, but it certainly is not true when the head is made smaller.

This is illustrated in the following table, where we have listed the percentage difference between the ratio of the flow times for two different solvents obtained at the highest head and the ratio obtained at the lowest head in one of the precursors of the viscometers described in this thesis. It was a normal Ubbelohde viscometer modified to the extent that it had a capillary going up and down and a bulb system with four bulbs, the effective hydrostatic head for the top bulb being 20 cm, for the lowest bulb, 3.93 cm.

Table

Percent Difference in the Ratio of the Flow Times Measured with Bulb I and Bulb II

System	benzene chloroform	toluene chloroform	water chloroform	water toluene	water McK
% Difference in flow time ratios	1.88	1.88	7.86	5.88	5.99

The surface tension of one organic liquid is very nearly the same as that of another, and is much smaller than the surface tension for water. Hence a viscometer designed to eliminate the surface tension effect with one organic liquid could serve equally well for other organic liquids but

not for water. Two series of viscometers were therefore designed, one (Series II) for organic liquids and the other (Series III) for water and aqueous solutions. The radius of curvature was chosen to make the correction zero for the lowest (fifth) bulb, since a surface tension effect will have most influence here. This meant that there was over-correction for the fourth and higher bulbs but the calibration showed that the effect of this over-correction on the measurement was negligible.

2. Design criteria for Series II.

Two viscometers were designed. Viscometer II-A, a low shear viscometer, covering the range 7.14 - 0.71 dynes/cm^2, and Viscometer II-B covering the range 17.9 - 2.38 dynes/cm^2 (calculated for benzene). It was necessary to design two viscometers, since the low range viscometer can cover only one decade. This range was just below the range usually covered. Therefore viscometer II-B was made to be able to extend the measurements to this range and also to provide overlap with II-A, in order to have a check on the consistency of the flow behaviour in this type of viscometer. The maximum shear stress obtainable in II-B is about as high as possible in a viscometer of this type which meets also our other requirements.

The flow times of the different bulbs were kept about

the same, by keeping the ratio h/V essentially constant.

3. Design criteria for Series III.

Only one viscometer was designed in this Series. The bulbs have all the same volume (1.48 ml). This was done for two reasons: (i) the surface tension correction is smaller the larger the bulb, (ii) if one was dealing with systems of varying surface tension, this effect could be calculated, and the correction applied to each bulb. The latter consideration was taken into account, because of the fact that many substances appreciably lower the surface tension of water, when dissolved in it. The shear stresses covered range from 6.25 to 0.94 Dyn/cm^2. The detailed design figures are listed in Table .

Chapter VI

EXPERIMENTAL WORK

A. Apparatus

(1) Viscometers

The viscometers II-A, II-B and III were used in the work to be described. They were mounted in stainless steel holders, equipped with a cylindrical pin which fitted snugly into a cylindrical slot in a stainless steel bar spanning the viscometer bath. This insured a reproducible, vertical position.

(2) Manostat

The manostat used was essentially the one described by Sones (61).

(3) Thermostats

Two baths of the aquarium type were used for the temperature range 20 - 40 C. These baths were filled with distilled water in order to discourage the growth of algae. For the 60 C work the bath was a cylindrical Pyrex Jar 18 inches high, filled with clear mineral oil and for the greater part insulated with asbestos. In both types of bath the temperature was maintained uniform by thorough stirring of the bath liquid and was maintained constant within 0.02 C

by means of a mercury thermoregulator operating through an electronic relay.

(4) Timers

Flow times were measured with two Heuer stop-watches (Catalog number 906). Times could be estimated to 0.03 seconds. The watches were periodically calibrated against an electronic time-calibrating device, by Messrs. Th. Lees and Co.

B. Materials

(1) Solvents

Benzene (Steel Co. of Canada) A.S.T.M. Industrial grade, redistilled and dried over sodium. B.P. 80.5 C

Toluene (Steel Co. of Canada) Nitration grade, redistilled and dried over sodium. B.P. 110 C

Methyl Ethyl Ketone (Shell Oil Co.) Technical grade, dried over anhydrous calcium sulphate ("Drierite") and redistilled. B.P. 79.8 C

Water. Ion exchange water was used.

All solvents, except water, were distilled through a three-foot column packed with glass helices. Condensate was rejected until the boiling point remained constant. One batch of solvent was used throughout a given series of viscosity determinations.

(2) Polymers

Dextran. The Dextran fraction used was supplied by Dr. Allene Jeanes (Northern Utilization Research Branch, U.S. Department of Agriculture, Peoria, Illinois). It had the following specifications:

	$[\eta]$	LINKAGES % 1-6	% 1-4	M_w	
Jeanes 3795-23	0.92	95	5	approx. 10×10^6	B-512-E

Poly(n-octyl-methacrylate). This fraction was supplied by Dr. S. Chinai (Plastics Research Section, Picatinny Arsenal, Dover, N.J.). Specifications:

	$[\eta]^{MEK}_{23°C}$	M_w
POMA-F1	2.75	$12.52 \times 10^{+6}$

Polystyrene. The Polystyrene used was fraction T-5, prepared and described by Sones ([61]) of this laboratory.

C. Experimental Procedure

1) Preparation of solutions. Solutions (in all solvents) were prepared at room temperature, by allowing the desired amount of polymer to dissolve slowly in the solvent in a 50 ml. volumetric flask (Exax). After complete dissolution the flasks were filled to the mark with solvent in a 20 C constant temperature bath.

Since the amount of polymer was small, the polymer was not weighed out in the flask but in a light-weight aluminium foil disk.

2) Determination of the concentration. Concentrations were calculated from the amount of polymer weighed out. At temperatures other than 20 C the concentration was calculated as

$$C_T = C_{25^\circ} \times \frac{d_o^T}{d_o^{25}} \qquad \text{(VI - 1)}$$

Tests carried out in this laboratory (58) have shown that using the density of the solvent in this calculation instead of the density of the solution introduces an error that is quite negligible.

All concentrations are expressed as grams/100 ml of solution. (g/100 ml) Dilutions in the viscometer were made with stock solvent kept in the 20 C constant temperature bath, the same pipette (Exax 5 ml) was used throughout all determinations.

3) Flow times. Flow times were measured in duplicate or triplicate. Flow times were rejected if they did not agree within 0.2 seconds.

With the multiple bulb viscometers, the same stopwatch was used with a given bulb throughout all determinations.

4) Calculation of true relative viscosities from the relative flow times. The relative viscosity is defined as

$$\eta_r = \frac{\eta_s}{\eta_o} = \frac{(\tau/a)_s}{(\tau/a)_o} \qquad \text{(VI - 2)}$$

s: solution
o: solvent

The assumption has been made that the kinetic energy effect has been eliminated. Then, at constant shear stress, we have

$$\eta_r = \frac{q_o}{q_s}$$

Or, if we consider the maximum shear stress at the wall

$$(\eta_r)_{\tau_R} = \left(\frac{q_o}{q_s}\right)_R \qquad \text{(VI - 3)}$$

The "nominal" rate of shear at the capillary wall is given as

$$q'_R = \tau_R \frac{1}{\eta_s}$$

The actual rate of shear at the capillary wall can be expressed as (5),

$$q_R = \frac{q'_R}{4}\left[3 + \frac{d\log q'_R}{d\log \tau_R}\right] \qquad \text{(VI - 4)}$$

The only assumption involved in (VI - 4) is that there exists a functional relationship between the rate of shear and the shear stress.

Substitution of (VI - 4) in (VI - 3), gives

$$(\eta_r)_{\tau_R} = \left(\frac{\tau_o}{q_s}\right)_R = \left(\frac{\tau_o}{q'_s}\right)_R \left[\frac{4}{3 + d\log q'_R / d\log \tau_R}\right]$$

Or

$$(\eta_r)_{\tau_R} = t_r \left[\frac{4}{3 + d\log q'_R / d\log \tau_R}\right] \qquad \text{(VI - 5)}$$

For Newtonian flow $\frac{d\log q'_R}{d\log \tau_R} = 1$ and hence $\eta_r = t_r$

For non-Newtonian flow $\frac{d\log q'_R}{d\log \tau_R} > 1$, hence $(\eta_r)_{\tau_R} < t_r$

Values of q'_R and τ_R were calculated from the measured flow times and plotted as Log q'_R vs Log τ_R. This plot was always linear and the derivative was evaluated as the slope of the least square fit to the line.

5) Calculation of the Intrinsic Viscosity. The intrinsic viscosity was evaluated from a plot of $\frac{\eta_r - 1}{c}$ and $\frac{\ln \eta_r}{c}$ vs c. Both $\frac{\eta_r - 1}{c}$ and $\frac{\ln \eta_r}{c}$ were calculated at four or five different concentrations. In all cases the plots were linear, and hence using the relationships

$$\frac{\eta_r - 1}{c} = [\eta] + k'[\eta]^2 c \qquad \text{(VI - 6)}$$

and:

$$\frac{\ln \eta_r}{c} = [\eta] - \beta [\eta]^2 c \qquad \text{(VI - 7)}$$

the intrinsic viscosity and the slope constant k' and β could be evaluated from a least square analysis.

It can be shown that β and k' are so related that their sum should be 0.50 ($\beta + k' = 0.50$). This relationship was never observed. Since the values of β were more reliable (internally consistent) than the values of k', the k' values were calculated from the β values assuming the theoretical relationship to be valid. This procedure is quite justified if one is not concerned with the values of k' but only with values relative to each other.

6. Determination of the Intrinsic Viscosity at Zero Shear Stress. Values of the intrinsic viscosity at finite shear stress were plotted against shear stress and the curve was extrapolated to a shear stress of zero.

D. Discussion of Experimental Results

1) Calibration of the viscometers.

a) Calibration of Series II. The calibration of Series II was performed by measuring the flow times of benzene and toluene at several different temperatures.

If we rewrite Poiseuille's equation in its condensed form, we have

$$\nu = At - \frac{B}{t} \qquad A = \frac{\pi R^4 hg}{8VL} \qquad B = mV/8\pi L$$

The viscometers were designed with a negligible kinetic energy correction, hence

$$\nu = At$$

If the surface tension effect has been eliminated, then the ratios of the flow times for different liquids for the same bulb should be equal to the ratios of the kinematic viscosity, and should be the same at different driving pressures (i.e. for different bulbs). This is indeed what was observed (see Table). The ratios of the flow times for benzene and toluene at 20° C ($t_{benzene}/t_{toluene}$), averaged over all ten bulbs is equal to 1.0929 $\pm$ 0.2%. The ratio of the kinematic

viscosities, as calculated from Timmerman's Tables ([67]) is equal to 1.1000. The agreement is considered to be satisfactory in view of the uncertainty in the literature values.

The constants A and B were evaluated for each bulb by means of the equation proposed by Higgins ([58]),

$$\frac{\nu}{t} = A - \frac{B}{t^2} \qquad \text{(VI - 8)}$$

The values for A and B, so calculated are listed in Table . If these values are known we can calculate the relative correction in the flow time, due to the kinetic energy correction, since it can be shown that it is equal to

$$\frac{\Delta t}{t} = B A / \nu^2 \qquad \text{(VI - 9)}$$

These values are also listed in Table .

Inspection of these values shows that the kinetic energy correction can be neglected. It should be noted that the values of the constant B are not proportional to the volume. This is attributed to a change in the value for m with driving pressure first observed by Swindells ([65]).

The volumes were measured by calibration with water, the geometrical head with a precision cathetometer. The length of the capillary was also measured, but this measurement is quite arbitrary, because of the trumpet-shaped ends of the capillary. These values, with the radius of the capillary

quoted by the makers of the precision bore tubing, enable us to calculate the constants A and B. Comparison with the actually observed values is satisfactory (see Table).

b) Calibration of Series III. Since this viscometer was designed for aqueous systems only, another calibration procedure was adopted. The flow times of water were measured with and without external pressure. Assuming no kinetic energy correction, the viscosity of water can be calculated from

$$\eta = \frac{\pi R^4}{8LV} p.t \qquad \text{(VI - 10)}$$

The calculated values were

Bulb	I	II	III	IV	V	Av.
$\eta^{25^\circ}_{H_2O}$	0.8910	0.8907	0.8908	0.8906	0.8906	0.8907

It is also possible to calculate the viscosity from a plot of the shear-stress vs 1/t, since

$$\tau = \frac{4V}{\pi R^3} \eta \frac{1}{t} \qquad \text{(VI - 11)}$$

The relationship, calculated for 35 points, obtained with external pressure only, is

$$\tau = 0.9866 \times 10^3 \cdot \frac{1}{t}$$

The viscosity of water, calculated from this relationship, is 0.8900 cp.

The constancy of these viscosity values, obtained over

a wide range of pressure heads proves that the surface tension correction has indeed been eliminated when the liquid is water. Furthermore it shows also that kinetic energy- and end-effects are negligible.

In order to determine to what extent the surface tension correction is eliminated for aqueous solutions for which the surface tension/density ratio is somewhat different than it is for water, another calibration was carried out with a 20% and with a 40% sucrose solution. These solutions are Newtonian liquids and hence the viscosity should be independent of the shear stress. Any change in the measured viscosity with a change in driving pressure would be due to a surface tension effect.

The viscosities calculated from the free fall data are

Bulb	I	II	III	IV	V
20%	1.696	1.700	1.703	1.708	1.723
40%	4.321	4.333	4.340	4.356	4.394

The increase in viscosity could be due to a surface tension effect. Since this effect amounts to a correction in the effective driving pressure, it should become negligible at higher hydrostatic heads. Therefore, measurements were made with external pressures on the 20% sucrose solution. The viscosities calculated from the pt vs 1/t plot were

Bulb	I	II	III	IV	V	Av.
20%	1.679	1.670	1.672	1.678	1.677	1.675

The increase in viscosity has disappeared, hence we may attribute the increase, noted in the free fall data, to a surface tension effect.

c) Summary and conclusion. From these calibration data we may then conclude that the design of the viscometers (of both Series) is sound and that they were constructed to specifications. They do indeed measure viscosities and the bothersome surface tension effect has been eliminated for all organic solvents in Series II and for water in Series III.

2) Use of the Viscometers in Typical Projects.

After calibration the viscometers were used in three different research projects, typical of those involving non-Newtonian liquids.

a) The intrinsic viscosity-molecular weight relationship. A neglect of the correction for shear effects will result in values of the intrinsic viscosity which are lower than they should be--and the discrepancy will be progressively larger at higher molecular weights. The plot of log $[\eta]$ vs log M will show a downward curvature in the high molecular weight range (see fig. III). Such a curvature may, however, also arise from chain-branching, since a branched molecule occupies a smaller volume than a linear molecule of the same molecular

weight (64). If a decrease in the intrinsic viscosity is to be used as evidence for, or a measure of, branching in a polymer, it is essential to find out whether all or part of the curvature is due to shear effects. Curvature of this type has been observed in the log $[\eta]$ vs log M plot in the systems Dextran - water (57) and in the system poly(n-octyl-methacrylate)-methylethylketone (11). We have therefore investigated the influence of shear stress on the intrinsic viscosity in these systems.

1) Measurements with a high molecular weight fraction of Dextran. Since shear effects are more marked in more concentrated solutions, measurements were made on a Dextran-water solution containing 0.9860 grams of Dextran per 100 ml of solution. The viscosity calculated from the free fall data were

Bulb	I	II	III	IV	Av.
	0.2832	0.2842	0.2842	0.2858	0.2845 $\pm$ .45%

The increase of 1% could be significant. In order to test this, measurements were also made with external pressure. The data were corrected for drainage according to the procedure described in Chapter III, plotting pt vs 1/t . The least square equations for the five bulbs are

Bulb	pt vs 1/t	calc. viscosity
I	$(pt)10^{-3} = 9554 - 0.3543 \times 10^5 \frac{1}{t}$	0.2845
II	$(pt)10^{-3} = 9576 - 0.3588 \times 10^5 \frac{1}{t}$	0.2851
III	$(pt)10^{-3} = 9555 - 0.3627 \times 10^5 \frac{1}{t}$	0.2852
IV	$(pt)10^{-3} = 9601 - 0.3839 \times 10^5 \frac{1}{t}$	0.2862
V	$(pt)10^{-3} = 9599 - 0.3980 \times 10^5 \frac{1}{t}$	0.2860
		Av. 0.2854 ($\pm$ .3%)

The calculated equations fitted the experimental points very well (better than 0.1%). As was pointed out in Chapter III the expression for the slope is

$$m \frac{dV^2}{\pi^2 R^4} - \frac{8LV\eta^2}{\pi R^4 d} - \frac{128}{5} \frac{V^2 L}{\pi^2 R^7} a_1$$

It is seen that the term representing the influence of the shear dependence is by far the largest. Substituting the actual values of the radius, volume and capillary length, we find a value of 0.298×10^{14} for this term. The value calculated from the least square analysis is found to be of the order of 10^8. Hence, if we attribute the observed slope to a shear effect, the coefficient a_1 is found to be of the order of 10^{-6}, which means that the effect of shear stress is negligible for shear stresses $< 10^2$, or shear rates $< 10^4$. Since the highest shear stress at free fall is 6.68 dynes/cm^2 we cannot attribute the increase of the viscosity to an effect of the shear stress.

We can conclude, therefore, that the curvature observed by Senti et al (57) is not due to shear effects and may be attributed to branching.

ii) Measurements with a high-molecular weight fraction of poly(n-octyl-methacrylate). The fraction was sent to us by Dr. S. N. Chinai in order to check whether any shear dependence of the intrinsic viscosity could be observed. Measurements were made in both Viscometers II-A and II-B. The data are recorded in Table XII and Fig. II . From these data an intrinsic viscosity at zero shear stress of 3.46 dl/gm was obtained by extrapolation, described in Chapter V. If this value of the intrinsic viscosity is plotted on the log vs log M plot, one observes that the correction for the effect of the shear dependence removes the curvature. Hence we may conclude that the poly(n-octyl-methacrylate) is essentially a linear molecule.

b) The Temperature Dependence of the Intrinsic Viscosity in a Good Solvent. According to Fox and Flory (22) the intrinsic viscosity of a polymer molecule can be expressed as

$$[\eta] = K M^{1/2} \alpha^3 \qquad \text{(VI - 12)}$$

with $K = \Phi \left[\frac{\overline{r_o^2}}{M}\right]^{3/2}$

$(\overline{r_o^2})^{1/2}$: root mean square end-to-end distance

M : mol. weight

Φ : Flory constant

and

$$\alpha^{5} - \alpha^{3} = 2 C_M \frac{1}{RT \bar{v}_2^2} (T\Delta S - \Delta H) M^{1/2}$$

$$C_M = \frac{27}{2^{2/5} \pi^{3/2}} \frac{\bar{v}^2}{N V_1} \left(\frac{\bar{r}_o^2}{M} \right)^{-3/2}$$

$\bar{v}$: spec. vol. of polymer

V_1: spec. vol. of solvent

ΔS: excess partial molar entropy of dilution

ΔH: excess partial molar heat of dilution

In a good solvent (ΔH negative), α is greater the more negative ΔH is. ΔH should become less negative as the temperature increases, hence α should decrease with temperature, unless K increases enough to compensate the decrease. The temperature dependence of K should, however, be very slight, since it depends only on the molecular weight, which is clearly independent of temperature, and the unperturbed root mean square end-to-end distance, which in principle is also not influenced by temperature.

In a poor solvent (ΔH positive), the intrinsic viscosity should increase with temperature, following a similar argument.

This behaviour is observed in many cases for low molecular weight polymers. Closer examination of the data reveals, however, that ΔH and ΔS are dependent on the molecular weight, a fact which is not considered in the Fox-Flory theory. It was noted (36), that as the molecular weight of the solute molecules increased, a solvent which could be considered good

for lower molecular weight molecules, became relatively poor. If this effect was real, it should be observable in the temperature dependence of the intrinsic viscosity. Since relatively high molecular weight polymers are required, to get a measurable effect, the solutions become non-Newtonian. The increase in intrinsic viscosity, measured at finite shear stress was already observed by Sharman ([68]) and Sones ([61]). Their data did not permit a reliable extrapolation to zero shear stress. With our low shear viscometers this is possible, and we therefore measured* the intrinsic viscosity of a high molecular weight fraction of polystyrene in toluene at three different temperatures in viscometers II-A and II-B. The data can be summarised as:

TABLE I

Polystyrene T5 in Toluene

Visc.	20°C		40°C		60°C	
	τ dynes/cm^2	$[\eta]$	dynes/cm^2	$[\eta]$	dynes/cm^2	$[\eta]$
II-A	4.55	9.32	4.52	9.38	4.35	9.45
	3.43	9.22	3.40	9.35	3.28	9.33
	2.32	9.12	2.30	9.13	2.22	9.20
	1.16	8.88	1.15	9.00	1.11	9.03
	.48	8.72	.48	8.84	.46	8.85
II-B	11.27	9.21	11.02	9.23	10.78	9.24
	7.51	8.94	7.35	8.93	7.18	8.87
	5.54	8.58	5.42	8.62	5.30	8.58
	3.37	8.36	3.30	8.40	3.22	8.34
	1.47	7.96	1.44	7.88	1.41	7.84

*The measurements were made by Mr. A. Tapajna, whose able assistance is very much appreciated.

From a plot of these intrinsic viscosities vs shear stress, we obtain for the intrinsic viscosity at zero shear stress:

	20°C	40°C	60°C
$[\eta]$	9.30	9.38	9.44

From these data it follows conclusively that the intrinsic viscosity at zero shear stress increases with temperature.

c) <u>The Influence of the Shear Stress on the Interaction Coefficient k'</u>. The interaction coefficient k' is defined by Huggins (17) as

$$\frac{\eta_r - 1}{c} = [\eta] + k'[\eta]^2 c \qquad \text{(VI - 13)}$$

The significance of this coefficient has been recently discussed by Frisch and Simha (23). It should be recognised that k' is a hydrodynamic interaction parameter. Any change in k' will be due to changes in hydrodynamic behaviour, whether induced by a change in solvent or, in non-Newtonian systems, by a change in shear stress. Theoretical calculations on the concentration dependence of the viscosity of suspensions lead to the following results

Particle Shape	k'	Reference
Sphere	0.745 1.17	with and without the effect of collisions
dumbell, rigid rod	0.77	Simha
rigid rod	0.73	Riseman and Ullman ( )
centrosymmetric flexible molecule	0.60	Riseman and Ullman ( )

We are interested not so much in the absolute magnitude of k' as in the changes in k'. From the data in the Table we can conclude that,

a) k' increases as the particle becomes more rigid or more asymmetric

b) k' decreases as the particle becomes more flexible.

It is assumed, throughout these calculations, that the particles are oriented at random. This raises the question how k' should be calculated in non-Newtonian systems, since at finite shear the orientation of the particles is no longer random. We will assume that at finite shear the Huggins' equation is valid for non-Newtonian liquids. Hence

$$\left(\frac{\eta_r - 1}{c}\right)_\tau = [\eta]_\tau + k'[\eta]_\tau^2 c \qquad \text{(VI - 14)}$$

Both k' and $[\eta]$ are functions of the shear stress. In order to eliminate the shear dependent variables, we will make the following substitution

$$[\eta]_\tau = [\eta]_0 (1 - \omega\tau^2)$$

Since the effect of the shear stress will be to make the particle more rigid and/or asymmetric, k' should be an increasing function of the shear stress, we will make the further assumption that it is a linear function of τ. Therefore,

$$k' = k'_0(1 + \beta\tau)$$

Making these substitutions we obtain

$$\left(\frac{\eta_r - 1}{c}\right)_\tau = [\eta]_o(1-\alpha\tau^2) + k'_o(1+\beta\tau)[\eta]_o^2(1-\alpha\tau^2)^2 c \qquad \text{(VI - 15)}$$

We have neglected, however, the inter-particle interaction. If, as seems reasonable, this interaction results in the formation of loose aggregates, it will itself be dependent on the shear stress, since at higher shear stresses the formation of these aggregates will be impeded. This interaction then will make a negative contribution to the concentration term $k' [\eta]^2 c$ and be proportional to the first power of the shear stress. Taking also inter-particle interaction into account we obtain

$$\left(\frac{\eta_r - 1}{c}\right)_\tau = [\eta]_o(1-\alpha\tau^2) + k'_o(1+\beta\tau)[\eta]_o^2(1-\alpha\tau^2)^2 c - \gamma\tau c \qquad \text{(VI - 16)}$$

This can be rewritten in a more manageable form if we define a new constant γ' , as

$$\gamma = \frac{\gamma'}{k'_o [\eta]_o^2}$$

Retaining only the linear and quadratic terms in the shear stress, we obtain as our final equation

$$\left(\frac{\eta_r - 1}{c}\right)_\tau = [\eta]_o(1-\alpha\tau^2) + k'_o [\eta]_o^2 (1 + (\beta - \gamma')\tau - 2\alpha\tau^2)c \qquad \text{(VI - 17)}$$

Since we are not interested in the contribution of the dependence of the intrinsic viscosity on the shear stress to the slope, but in the dependence of k' on τ , we will divide

the slope by $[\eta]_\tau$.

Hence we obtain the quantity

$$k'_o [1 + (\beta - \gamma)\tau_c]$$

From this it is clear that k'_o can be obtained by extrapolation of this quantity to zero shear stress. This plot is shown in fig. .

No dependence on the shear stress is observed at 20°C, which can be interpreted by the fact that the increase of k' with shear stress is offset by inter-particle interaction. The increase observed at 40° and 60°C can be attributed to an increased rigidity and asymmetry of the molecule at higher shear stresses; the decrease of k' with temperature to an increased flexibility.

A similar increase in k' was observed by Kuroiwa (34) in solutions of polystyrene in toluene, but no explanation was put forward to account for this.

TABLES

TABLE II

Specifications for Variable Shear Viscometer II-A

capillary radius R = 0.025 cm capillary length L = 50 cm (2x25)
radius of curvature of hemispherical opening R_o = 0.37 cm

Bulb	I	II	III	IV	V
h (cm)	20	15	10	5	2
V (cm^3)	1.5	1.12	0.75	0.40	0.30
r_{bulb}(cm)	.710	.644	.564	.457	.415
A x 10^{-5}	4.01	4.03	4.01	3.76	1.99
B x 10^{-2}	.133	.100	.067	.036	.026
$t_{Benzene}$	171.2	170.4	171.2	182.6	345.1

TABLE III

Specifications for Variable Shear Viscometer II-B

capillary radius R = 0.025 cm capillary length L = 30 cm (2x15)
radius of curvature of hemispherical opening R_o = 0.413 cm

Bulb	I	II	III	IV	V
h (cm)	30	20	15	9	4
V (cm^3)	3.0	2.0	1.50	.90	.40
r_{bulb}(cm)	.90	.78	.71	.59	.46
A x 10^{-5}	5.00	5.00	5.00	5.00	5.00
B x 10^{-2}	.446	.297	.223	.134	.059
$t_{Benzene}$(sec)	137	137	137	137	137

TABLE IV

Specifications for Variable Shear Viscometer III

capillary radius R = 0.025 cm capillary length L = 40 cm (2x20)
radius of curvature of hemispherical opening R_o = 0.64 cm

Bulb	I	II	III	IV	V
h (cm)	20	15	10	5	3
V (cm^3)	1.50	1.50	1.50	1.50	1.50
r_{bulb}(cm)	0.70	0.70	0.70	0.70	0.70
A x 10^{-5}	5.00	3.75	2.50	1.25	0.75
B x 10^{-2}	.167	.167	.167	.167	.167
b_{water}(sec)	200	266	400	800	1330

TABLE V

Flow Times of Benzene and Toluene at Various Temperatures

Viscometer II-A

Bulb	Benzene 20°	Benzene 25°	Toluene 20°	Toluene 40°	Toluene 60°
I	147.99	138.40	135.44	110.07	92.60
II	148.27	138.73	135.78	110.31	92.65
III	147.20	137.50	134.43	109.25	91.72
IV	161.48	151.23	147.72	119.41	100.33
V	294.78	275.41	269.03	215.58	181.82

Viscometer II-B

Bulb	Benzene 20°	Benzene 40°	Toluene 20°	Toluene 40°	Toluene 60°
I	134.36	105.01	123.08	110.07	84.37
II	133.78	104.50	122.44	110.31	83.68
III	137.07	107.05	125.48	109.25	85.51
IV	134.63	105.40	123.16	119.41	83.70
V	142.70	112.48	130.83	215.58	88.22

TABLE VI

Calibration Constants from Higgins' Plot

Viscometer II-A

Bulb	A x 10^{-5}	B x 10^{-2}	AB x 10^{-7}	K.E. corr. for a liquid with $\nu = 10^{-2}$ C.Stokes
I	5.025	0.621	3.12	.31%
II	5.008	0.516	2.58	.26%
III	5.049	0.101	0.51	.05%
IV	4.583	0.094	0.43	.04%
V	2.503	0.093	0.23	.02%

Viscometer II-B

Bulb	A x 10^{-5}	B x 10^{-2}	AB x 10^{-7}	K.E. corr. for a liquid with $\nu = 10^{-2}$ C.Stokes
I	5.555	1.196	6.64	.66%
II	5.563	0.929	5.17	.52%
III	5.416	0.752	4.07	.41%
IV	5.497	0.520	2.86	.29%
V	5.144	0.066	.34	.03%

TABLE VII

Flow Times of Water at 20°C at Various Shear Stresses in Viscometer III

Bulb	t(sec)	τ (dynes/cm^2)	t(sec)	τ (dynes/cm^2)	t(sec)	τ (dynes/cm^2)	t(sec)	τ (dynes/cm^2)
I	147.78	6.68	89.39	11.04	65.71	14.94	50.29	19.45
II	198.59	4.78	106.32	9.33	74.26	13.24	55.22	17.74
III	296.24	3.33	128.46	7.68	84.38	11.59	60.64	16.09
IV	487.61	2.03	154.46	6.38	95.32	10.29	66.11	14.79
V	912.35	1.08	181.06	5.43	104.93	9.34	70.56	13.85

Bulb	t(sec)	τ (dynes/cm^2)	t(sec)	τ (dynes/cm^2)	t(sec)	τ (dynes/cm^2)	t(sec)	τ (dynes/cm^2)
I	34.76	29.30	28.91	33.97	25.42	38.83	21.73	45.32
II	36.93	26.57	30.35	32.26	26.47	37.12	22.51	43.61
III	39.19	24.92	31.82	30.62	27.76	35.47	23.38	41.97
IV	41.50	23.63	33.47	29.32	28.90	34.17	24.43	40.67
V	43.08	22.66	34.48	28.35	29.60	33.21	24.85	39.59

TABLE VIII

Flow Times of 20% and 40% Sucrose Solutions
Without External Pressure

Bulb	20% Sucrose	40% Sucrose
I	260.61	716.8
II	351.0	965.9
III	524.3	144.3
IV	865.8	238.4
V	163.3	450.1

TABLE IX

Flow Times of a 20% Sucrose Solution at Various Shear Stresses

Bulb	t(sec)	τ (dynes/cm^2)	t(sec)	τ (dynes/cm^2)	t(sec)	τ (dynes/cm^2)
I	260.64	7.22	122.74	15.14	94.72	19.67
II	351.01	5.37	139.79	13.30	104.11	17.82
III	524.32	3.60	160.7	11.52	115.56	16.04
IV	865.80	2.19	183.32	10.11	126.95	14.63
V	1633.8	1.17	203.76	9.09	136.66	13.62

Bulb	t(sec)	τ (dynes/cm^2)	t(sec)	τ (dynes/cm^2)	t(sec)	τ (dynes/cm^2)	t(sec)	τ (dynes/cm^2)
I	66.36	28.07	55.02	33.86	48.13	38.65	41.05	45.18
II	71.00	26.23	58.09	32.02	50.60	36.80	43.05	43.33
III	75.68	24.45	61.26	30.24	52.94	35.02	44.45	41.55
IV	80.85	23.04	64.52	28.83	55.20	33.61	46.32	40.15
V	84.51	22.02	66.82	27.81	57.09	32.60	47.60	39.13

TABLE X

Calibrated Dimensions of Viscometers II-A, II-B and III

Viscometer II-A

capillary radius R = 0.0267 capillary length: 50.90 cm

Bulb	I	II	III	IV	V
h (cm)	20.42	15.38	10.39	5.23	2.17
V (cm^3)	1.573	1.187	0.794	0.439	0.332
A x 10^{-5}	5.025	5.008	5.049	4.583	2.503
B x 10^{-2}	0.621	0.516	0.101	0.094	0.093
$t_{Benzene}$ $20^{o}C$(sec)	147.99	148.27	147.20	161.48	294.78

Viscometer II-B

capillary radius R = 0.0256 capillary length: 30.35 cm

Bulb	I	II	III	IV	V
h (cm)	31.38	20.92	15.43	9.37	4.10
V (cm^3)	3.144	2.086	1.573	0.936	0.434
A x 10^{-5}	5.555	5.563	5.416	5.497	5.144
B x 10^{-2}	1.196	0.929	0.752	0.520	0.066
$t_{Benzene}$ $20^{o}C$(sec)	134.36	133.78	137.07	134.63	142.70

continued

TABLE X - continued

Viscometer III

capillary radius r = 0.0263 capillary length: 39.78 cm

Bulb	I	II	III	IV	V
h (cm)	20.68	15.35	10.27	6.22	3.27
V (cm^3)	1.584	1.585	1.581	1.584	1.583
A x 10^{-5}	6.05	4.49	3.00	1.82	0.95
t_{water} 25°C	148.26	199.70	298.36	493.06	938.69

TABLE XI

Flow Times of a Solution of a High Molecular Weight Fraction of Dextran at Various Shear Stresses

Bulb	t(sec)	τ dynes/cm^2	t(sec)	τ dynes/cm^2	t(sec)	τ dynes/cm^2
I	469.65	7.22	210.76	14.71	159.78	19.30
II	633.64	5.37	240.13	13.00	175.84	17.59
III	947.27	3.60	274.72	11.35	194.16	15.94
IV	1564.5	1.17	312.19	10.05	212.25	14.64
V	-	-	345.19	9.08	227.56	13.67

Bulb	t(sec)	τ dynes/cm^2	t(sec)	τ dynes/cm^2	t(sec)	τ dynes/cm^2
I	90.57	33.5	78.74	38.25	66.75	44.71
II	95.77	31.8	82.82	36.53	69.63	43.00
III	100.99	30.1	86.62	34.88	72.34	41.35
IV	106.02	28.8	90.42	33.59	74.94	40.06
V	109.54	27.9	93.02	32.62	76.81	39.09

TABLE XII

Intrinsic Viscosity of Poly(n-octyl-methacrylate) --(POMA - F_1)--at 23°C in Methyl Ethyl Ketone in Viscometer II-A

Bulb	C	t_r	η_r	$\ln \eta_r/c$	$[\eta]$
I	0.2049	1.861	1.858	3.023	3.28
τ = 421	0.1639	1.659	1.657	3.082	
dynes/cm^2	0.1366	1.533	1.530	3.113	β = .12
	0.1171	1.446	1.444	3.137	
	0.1024	1.384	1.382	3.160	
II					
τ = 3.17		1.873	1.870	3.055	3.34
dynes/cm^2		1.669	1.666	3.118	
		1.541	1.539	3.156	β = .13
		1.453	1.451	3.187	
		1.390	1.388	3.203	
III					
τ = 2.14		1.882	1.878	3.076	3.39
dynes /cm^2		1.676	1.673	3.140	
		1.547	1.545	3.184	
		1.466	1.456	3.209	β = .14
		1.395	1.393	3.239	
IV					
τ = 1.07		1.893	1.890	3.107	3.45
dynes/cm^2		1.686	1.683	3.176	
		1.555	1.553	3.222	
		1.466	1.464	3.255	β = .14
		1.401	1.399	3.281	
V					
τ = .446		1.895	1.892	3.112	3.43
dynes/cm^2		1.688	1.686	3.187	
		1.554	1.551	3.213	
		1.465	1.464	3.255	β = .14
		1.401	1.399	3.281	

TABLE XIII

Intrinsic Viscosity of Poly(n-octyl-methacrylate) --(POMA - F_1)--at 23°C in Methyl Ethyl Ketone in Viscometer II-B

Bulb	C	t_r	η_r	$\ln\eta_r/c$	$[\eta]$
I	0.2049	1.814	1.806	2.884	3.06
$\tau = 10.42$ dynes/cm^2	0.1639	1.622	1.616	2.927	
	0.1366	1.503	1.497	2.955	$\beta = .09$
	0.1171	1.420	1.415	2.964	
	0.1024	1.360	1.356	2.974	
II		1.846	1.837	2.968	3.20
$\tau = 6.94$ dynes/cm^2		1.647	1.641	3.022	
		1.524	1.517	3.050	
		1.440	1.435	3.084	$\beta = .11$
		1.375	1.371	3.081	
III		1.861	1.852	3.008	3.26
$\tau = 5.12$ dynes/cm^2		1.658	1.652	3.063	
		1.533	1.526	3.094	$\beta = .12$
		1.447	1.442	3.125	
		1.384	1.380	3.132	
IV		1.873	1.865	3.042	3.31
$\tau = 3.12$ dynes/cm^2		1.668	1.662	3.099	
		1.539	1.532	3.123	
		1.455	1.445	3.143	$\beta = .12$
		1.390	1.385	3.182	
V		1.882	1.874	3.065	3.40
$\tau = 1.36$ dynes/cm^2		1.673	1.667	3.118	
		1.561	1.554	3.228	
		1.463	1.458	3.221	$\beta = .14$
		1.395	1.391	3.223	

TABLE XIV

Intrinsic Viscosity of PS T5 at 40°C in Viscometer II-A

Bulb	C	t_r	η_r	$\ln\eta_r/c$	$[\eta]$
I	.0681	1.724	1.723	8.022	8.86
$\tau = 4.52_2$	.0511	1.524	1.522	8.219	
dynes/cm^2	.0409	1.407	1.406	8.330	$\beta = .15$
	.0340	1.335	1.335	8.497	
II		1.739	1.737	8.107	9.00
$\tau = 3.40_2$		1.533	1.530	8.323	
dynes/cm^2		1.415	1.413	8.452	$\beta = .15$
		1.339	1.339	8.585	
III		1.752	1.751	8.226	9.14
$\tau = 2.30_2$		1.545	1.541	8.462	
dynes/cm^2		1.424	1.422	8.608	$\beta = .16$
		1.346	1.345	8.718	
IV					
$\tau = 1.15_2$		1.766	1.765	8.344	9.36
dynes/cm^2		1.555	1.550	8.589	
		1.431	1.430	8.751	$\beta = .17$
		1.352	1.352	8.871	
V		1.771	1.770	8.385	9.38
$\tau = 0.48_2$		1.557	1.551	8.640	
dynes/cm^2		1.433	1.433	8.797	
		1.354	1.354	8.915	$\beta = .17$

TABLE XV

Intrinsic Viscosity of PS T5 tol. at 40°C
in Viscometer II-B

Bulb	C	t_r	η_r	$\ln\eta_{r/c}$	$[\eta]$
I	.0681	1.661	1.649	7.345	7.90
$\tau = 11.02$ dynes/cm^2	.0511	1.475	1.466	7.487	
	.0409	1.369	1.362	7.555	$\beta = .14$
	.0340	1.302	1.297	7.653	
II		1.698	1.686	7.671	8.38
$\tau = 7.35_2$ dynes/cm^2		1.502	1.493	7.845	
		1.391	1.384	7.949	$\beta = .15$
		1.320	1.314	8.029	
III		1.720	1.708	7.800	8.64
$\tau = 5.42_2$ dynes/cm^2		1.518	1.508	8.037	
		1.402	1.396	8.159	$\beta = .17$
		1.329	1.323	8.229	
IV		1.746	1.733	8.073	8.91
$\tau = 3.30_2$ dynes/cm^2		1.536	1.527	8.282	
		1.417	1.410	8.401	$\beta = .15$
		1.341	1.335	8.497	
V		1.765	1.752	8.233	9.23
$\tau = 1.44_2$ dynes/cm^2		1.550	1.541	8.462	
		1.428	1.421	8.592	$\beta = .16$
		1.351	1.345	8.718	

TABLE XVI

Intrinsic Viscosity of [ ] PS T5 tol. at 60°C
in Viscometer II-A

Bulb	C	t_r	η_r	$\ln\eta_{r/c}$	$[\eta]$
I	.0568	1.567	1.563	7.819	8.80
$\tau = 4.35_2$	.0426	1.417	1.414	8.056	
dynes/cm^2	.0340	1.327	1.325	8.185	
	.0284	1.271	1.269	8.306	$\beta = .18$
II		1.578	1.574	7.942	8.96
$\tau = 3.28_2$		1.424	1.421	8.171	
dynes/cm^2		1.333	1.331	8.338	
		1.276	1.274	8.444	$\beta = .19$
III		1.588	1.584	8.044	9.10
$\tau = 2.22_2$		1.433	1.430	8.321	
dynes/cm^2		1.340	1.338	8.497	
		1.280	1.278	8.556	$\beta = .20$
IV		1.598	1.594	8.164	9.27
$\tau = 1.11_2$		1.440	1.437	8.452	
dynes/cm^2		1.344	1.344	8.562	
		1.285	1.283	8.722	$\beta = .20$
V		1.605	1.600	8.232	9.44
$\tau = 0.46_2$		1.446	1.443	8.534	
dynes/cm^2		1.349	1.347	8.697	
		1.289	1.287	8.806	$\beta = .21$

TABLE XVII

Intrinsic Viscosity of [ ] PS T5 tol. at 60°C
in Viscometer II-B

Bulb	C	t_r	η_r	$\ln\eta_r/c$	$[\eta]$
I	.0568	1.518	1.509	7.255	7.84
τ = 10.78	.0426	1.377	1.369	7.381	
dynes/cm^2	.0340	1.295	1.289	7.488	β = .10
	.0284	1.243	1.238	7.542	
II		1.547	1.538	7.590	8.28
τ = 7.18$_2$		1.399	1.392	7.756	
dynes/cm^2		1.313	1.307	7.891	β = .13
		1.258	1.253	7.940	
III		1.565	1.556	7.796	8.56
τ = 5.30$_2$		1.410	1.403	7.955	
dynes/cm^2		1.323	1.317	8.094	β = .15
		1.266	1.261	8.194	
IV		1.584	1.575	8.010	8.86
τ = 3.22$_2$		1.426	1.418	8.204	
dynes/cm^2		1.333	1.327	8.318	
		1.275	1.270	8.444	β = .16
V		1.593	1.583	8.098	9.25
τ = 1.41$_2$		1.435	1.428	8.291	
dynes/cm^2		1.343	1.337	8.562	
		1.282	1.277	8.641	β = .18

TABLE XVIII

Intrinsic Viscosity of P-S T_5 in Toluene at 20° C.
in Viscometer II-A

Bulb	C	t_r	η_r	$\ln\eta_r/c$	$[\eta]$
I					
τ = 4.55 dynes/cm^2	.0626	1.639	1.635	7.853	8.72
	.0470	1.463	1.461	8.066	
	.0376	1.362	1.360	8.178	β = .18
	.0313	1.297	1.296	8.287	
II					
τ = 3.43 dynes/cm^2		1.651	1.647	7.955	8.88
		1.471	1.469	8.185	
		1.369	1.367	8.316	
		1.302	1.301	8.431	β = .19
III					
τ = 2.32 dynes/cm^2		1.668	1.664	8.134	9.12
		1.485	1.483	8.385	
		1.378	1.376	8.489	
		1.311	1.310	8.626	β = .15
IV					
τ = 1.16 dynes/cm^2		1.678	1.674	8.230	9.22
		1.492	1.489	8.474	
		1.384	1.382	8.606	β = .17
		1.314	1.312	8.674	
V					
τ = .48 dynes/cm^2		1.688	1.683	8.316	9.32
		1.499	1.496	8.574	
		1.388	1.386	8.683	β = .19
		1.318	1.317	8.792	

TABLE XIX

Intrinsic Viscosity of P-S T_5 in Toluene at 20° C. in Viscometer II-B

Bulb	C	t_r	η_r	$\ln\eta_r/c$	$[\eta]$
I					
τ = 11.27 dynes/cm^2	.0626	1.584	1.573	7.236	7.96
	.0470	1.425	1.417	7.415	
	.0376	1.333	1.326	7.500	β = .18
	.0313	1.272	1.268	7.588	
II					
τ = 7.51 dynes/cm^2		1.615	1.604	7.546	8.36
		1.446	1.438	7.730	
		1.350	1.344	7.864	β = .18
		1.287	1.282	7.907	
III					
τ = 5.54 dynes/cm^2		1.634	1.623	7.735	8.58
		1.460	1.452	7.936	
		1.360	1.354	8.061	
		1.295	1.290	8.205	β = .18
IV					
τ = 3.37 dynes/cm^2		1.660	1.648	7.981	8.94
		1.479	1.471	8.212	
		1.375	1.369	8.356	β = .18
		1.307	1.302	8.431	
V					
τ = 1.47 dynes/cm^2		1.680	1.668	8.174	9.21
		1.494	1.486	8.429	
		1.388	1.382	8.606	β = .19
		1.317	1.312	8.674	

BIBLIOGRAPHY

1. Akkerman, F.; Pals, D.T.F.; Hermans, J.J. Rec. Trav. Chim. Pays. Bas. 71, 56-63 (1952).

2. Barr, G. A Monograph of Viscometry. New York: Humphrey Milford, 1931.

3. --------. Proc. Phys. Soc. London. 58 (1946), 575.

4. Bashforth, F. and Adams, J.C. Capillary Action. Cambridge: University Press, 1883.

5. Bestul, A.B. and Belcher, H.V. J. Colloid Sc., 5 (1950), 303-314.

6. Bigelow, C.C. Ph.D. Thesis, McMaster University, 1957.

7. Bingham. Fluidity and Plasticity. New York: McGraw-Hill Book Co. Inc., 1922.

8. Bueche, F. J. Chem. Phys., 22 (1954), 1510.

9. Cerf, R. J. Polymer Sc., 23 (1957), 125-150.

10. --------. J. Physique et le Radium, 19 (1958), 127-134.

11. Chinai, S. N. Private communication.

12. Chandrashecar, R.

13. Copick, M. J. Chim. Phys., 53 (1956), 440-444.

14. Davies, C. N. Proc. Intern. Rheol. Congress, Holland, (1948), page III - 47.

15. Dean

16. --------

17. De Wind, G. and Hermans, J.J. Rec. Trav. Chim. des Pays Bas, 70 (1951), 521-536.

18. Edelmann, K. Simp. Internaz. Chimica Macromol. (1955) 3-15.

19. Eisenberg, H. J. Polymer Sc., 25 (1957), 257-271.

20. Eyring, H. J. Chem. Phys., 4 (1936), 283.

21. First Report on Viscosity and Plasticity. Amsterdam: Noord-Hollandse Uitgevers Maatschappij. P.125.

22. Flory, P.J. and Fox Jr., T.G. J. Am. Chem. Soc., 73 (1951), 1904.

23. Frisch, H. L. and Simha, R. "The Viscosity of Colloidal Suspensions and Macromolecular Solutions", Chapter 14 in Rheology, Vol. 1, ed. Eirich. Academia 1956.

24. Fuoss, R.M. and Cathers, G.I. J. Polymer Sc., 6 (1949), 97-120.

25. Garner, F.H.; Nissan, A.H. and Wood, G.F. Phil. Trans. Roy. Soc. London, A, 243 (1950), 37-66.

26. Hermans Jr., J. Ph.D. Thesis, Leyden, 1958.

27. Huggins, M.L. J. Chem. Phys.

28. Ikeda, Y. J. Phys. Soc. Japan, 12 (1957), 378-384.

29. Kirkwood, J. G. Proc. Inter. Coll. on Macromol. Amsterdam, 1949, p. 133.

30. Kirkwood, J.G. and Plock, R.J. J. Chem. Phys., 24 (1956), 665-669.

31. Kooi, J. Ph.D. Thesis, Groningen, 1952.

32. Krigbaum, W. R. and Flory, P. J. J. Polymer Sc., 11 (1953), 37.

33. Kuhn, W. and Kuhn, H. Helv. Chim. Acta, 28 (1945), 1533.

34. Kuroiwa, T. Bull. Chem. Soc. Japan, 29 (1956), 164-169.

35. Lodge, A. S. Trans. Far. Soc., 52 (1956), 120-130.

36. Manson, J. A. M.Sc. Thesis, McMaster University, 1951.

37. Markovitz, H. Trans. Soc. Rheology, 1 (1957), 37-52.

38. Maron, S. H.; Krieger, I.M. and Sisko, A.W. J. Appl. Phys., 25 (1954), 971-976.

39. Ohrn, Olove. J. Polymer Sc., 17 (1955), 137.

40. Oldroyd, J.G. Quart. J. Mech. Appl. Math., 4 (1951), 271.

41. --------. "Non-Newtonian Flow of Liquids and Solids", in Rheology, Vol. I, Chap. 12, ed. F. R. Eirich. Academia Press, 1956.

42. Ostwald, W. Kolloid L., 36 (1925), 99.

43. Peterlin, A. Journal of Polymer Sc., 8 (1952), 621.

44. Peterlin, A. and Copick, M. J. Appl. Phys., 27 (1956), 434-438.

45. Philippoff, W. Viskositat der Colloide. Verlag: Theodor Skinkopff, 1942.

46. Prandtl and Vandrey. Z. angew. Math. Mech., 30 (1950), 169.

47. Ree, T. and Eyring, H. J. Appl. Phys., 26 (1955), 800-809.

48. --------. "The Relaxation Theory of Transport Phenomena", in Rheology, Vol. II, Chap. 3, ed. F. R. Eirich. Academia Press, 1958.

49. Reiner, M. Deformation and Flow. London: H. K. Lewis & Co. Ltd., 1949.

50. Rouse Jr., P.E. J. Chem. Phys., 21 (1953), 1272.

51. Scheraga, H.A. J. Chem. Phys., 23 (1955), 1526-1532.

52. Schultz-Grunow, F. and Weymann, H. Kolloid Z., 131 (1953), 61-66.

53. Schurz, J. and Immergut, E.H. J. Polymer Sc., 9 (1952), 279.

54. Schurz, J. Kolloid. Z., 154 (1957), 97.

55. --------. Kolloid. Z., 155 (1957), 45, 55.

56. --------. Rheologica Acta, 1 (1958), 58-63.

57. Senti, F.R.; Hellman, N.N.; Ludwig, N.H.; Babcock, G.E.; Tobin, R.; Glass, C.A. and Lamberts, B.L. J. Polymer Sc., 27 (1955), 527-546.

58. Sharman, L.J. M.Sc. Thesis, McMaster University, 1951.

59. Signer, R. Zeit. für Physitalische Chem. (A), 150 (1930), 257.

60. Signer, R. and Berneis, K. Makromol. Chem., 8 (1952), 268-282.

61. Sones, R.H. M.Sc. Thesis, McMaster University, 1952.

62. Sprokel, G.J.M. Ph.D. Thesis, Utrecht, 1952.

63. Staudinger, H. Hochmolecular Organische Verbindungen. Julius Springer Verlag (1932).

64. Stockmayer, W.H. and Fixman, M. Am. New York Acad. Sc., 57 (1953), 334-352.

65. Swindells, J.F.; Hardy, R.C. and Cottington, R.L. J. Res. Natl. Bur. Stand., 52 (1954), 105-120.

66. ---------. Private communication.

67. Timmermans

68. Toms, B.A. and Strawbridge, D.J. Proc. 2nd Intern. Rheol. Congr., Oxford, 1953, p. 99.

69. Tuynman, C.A.F. Ph.D. Thesis, Leyden, 1956.

70. Ubbelohde, L. J. Inst. Petr. Techn., 23 (1937), 427-451.

71. Umstätter, H. Strukturmechanik. Theodor Steinkopff, 1948.

72. Wada, E. J. Scient. Res. Inst. Japan, 47 (1953), 47, 159.

73. Weymann, H. Kolloid. Zeit., 138 (1954), 41-56.

74. Yoh-Han Pao. J. Chem. Phys., 25 (1956), 1294.

75. Zimm, B.H. J. Chem. Phys., 24 (1956), 269-278.

A : Filling tube
O.D : 1 cm

B : Bulb system

C : Air inlet tube
O.D : 0.6 cm

F : O.D : 0.6 cm
I.D : 0.4 cm

F almost touches the bottom of dilution-bulb.

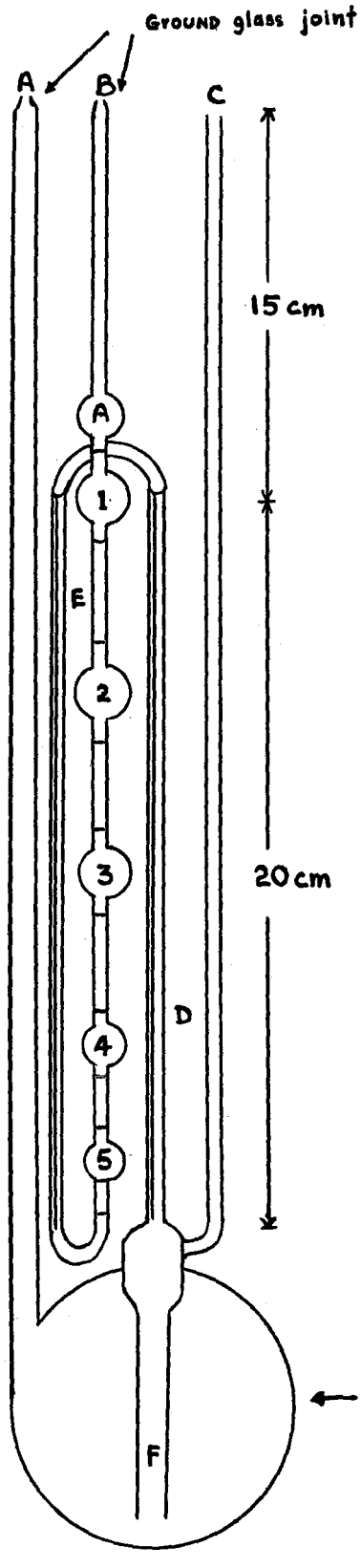

Horizontal Cross section

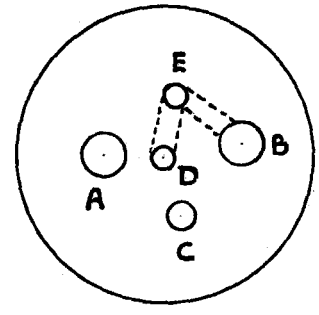

Modified Ubbelohde Shear Viscometer

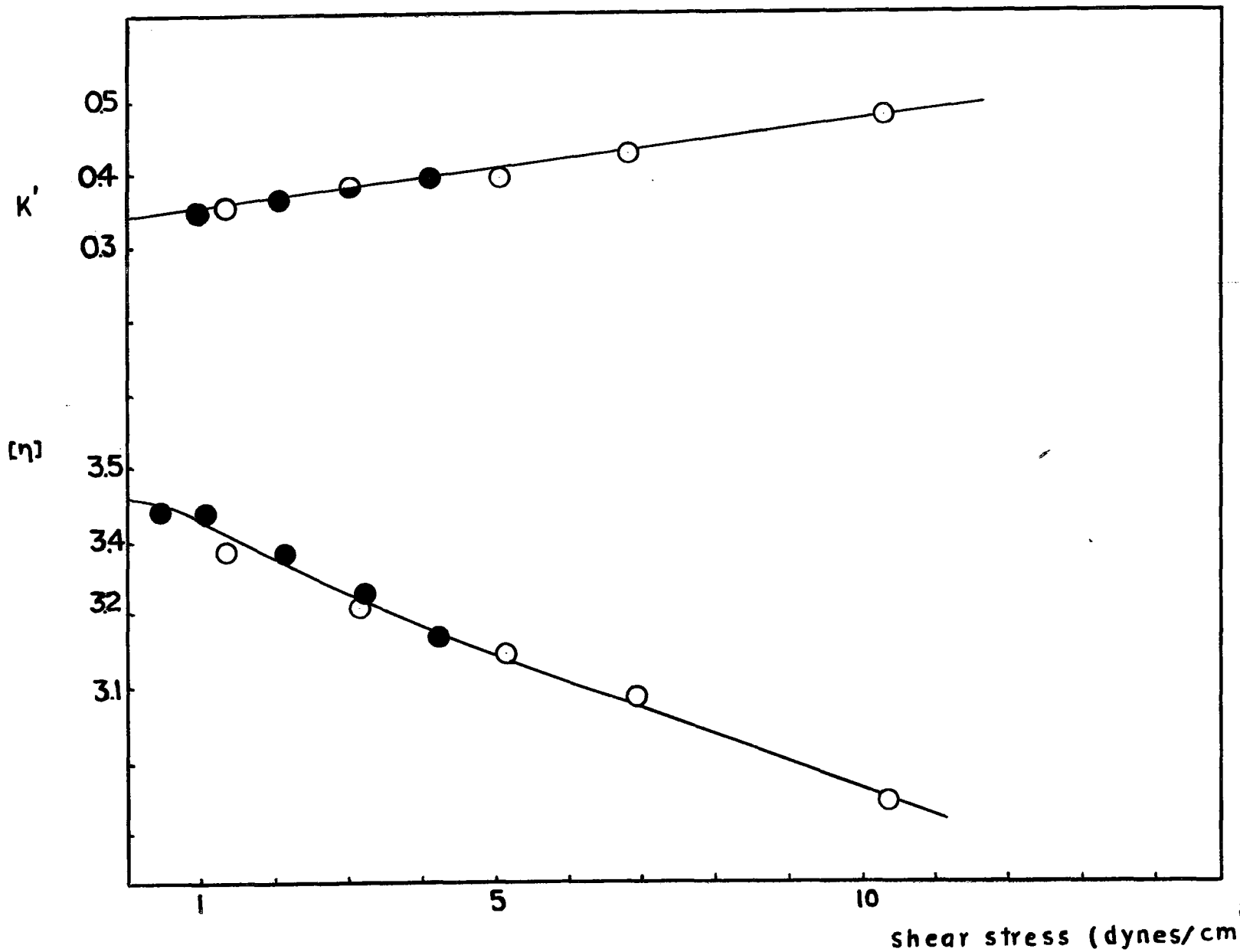

Fig II

Dependence of the Intrinsic Viscosity and K' on Shear Stress for Poma F1 in MEK

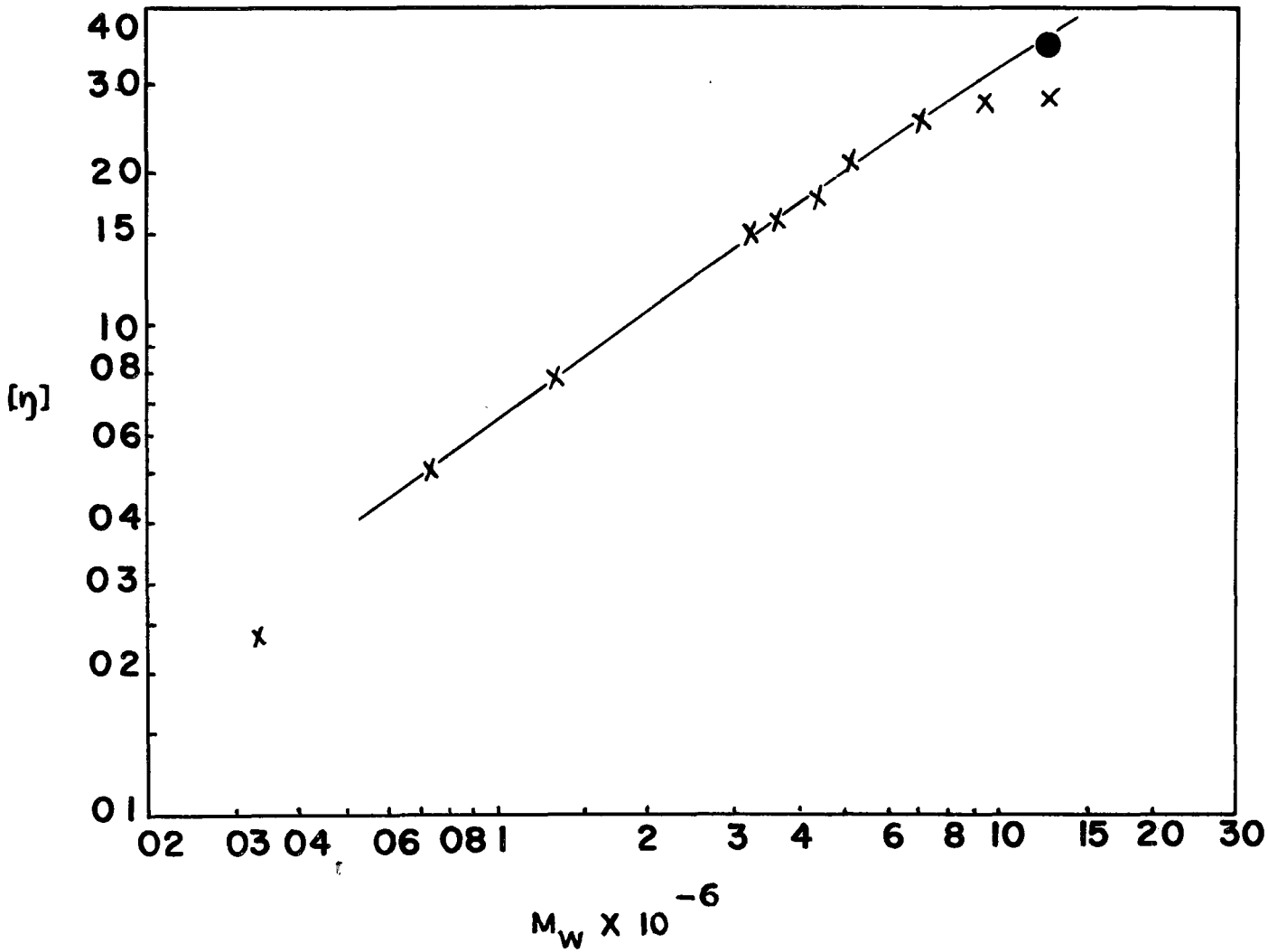

Relation between Intrinsic Viscosity and Molecular Weight for Poly-n-octyl Methacrylate in Methyl Ethyl Ketone

Fig III

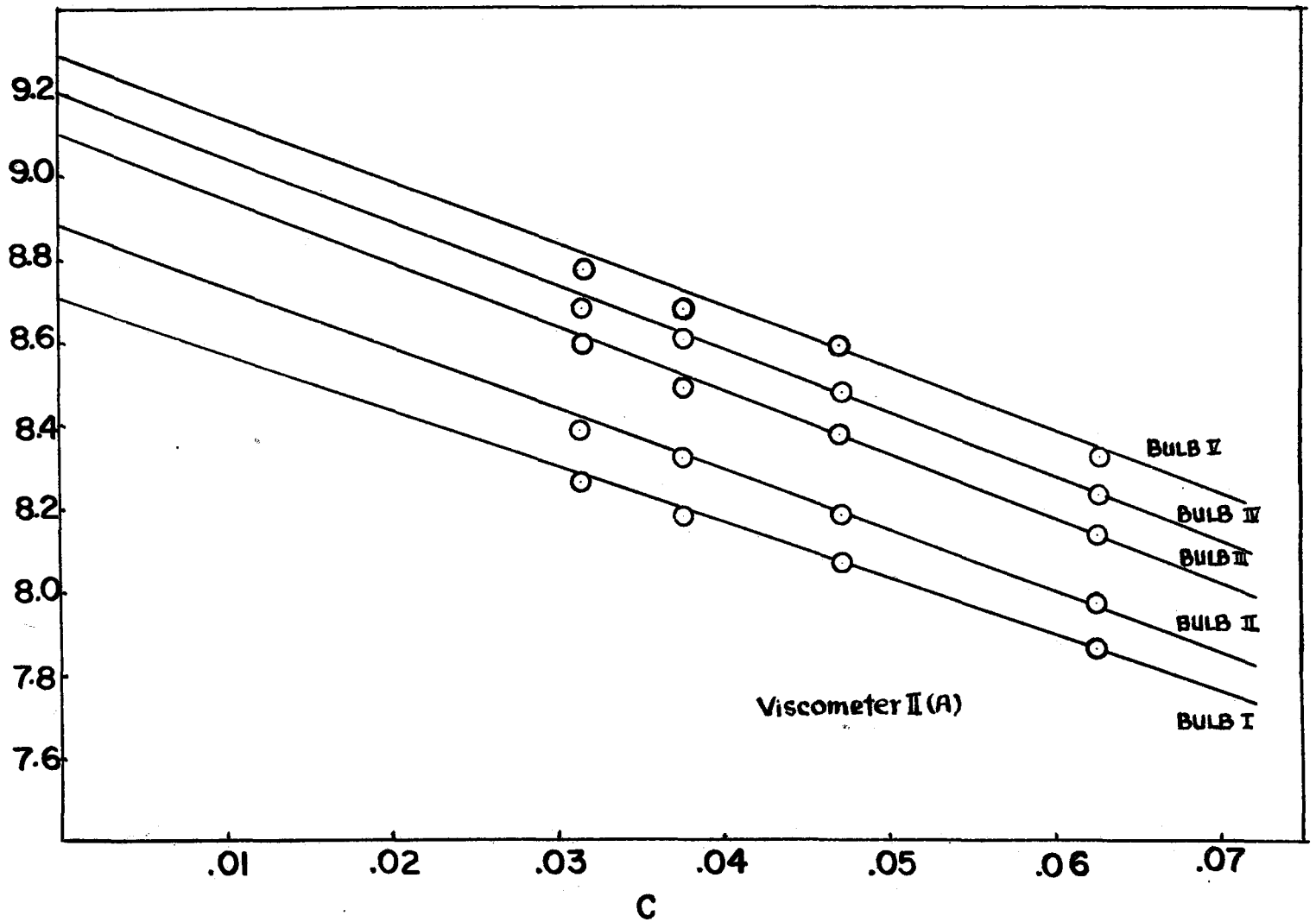

Inherent Viscosity vs Concentration Plot of Polystylene T in Toluene at 20° C

Fig 2

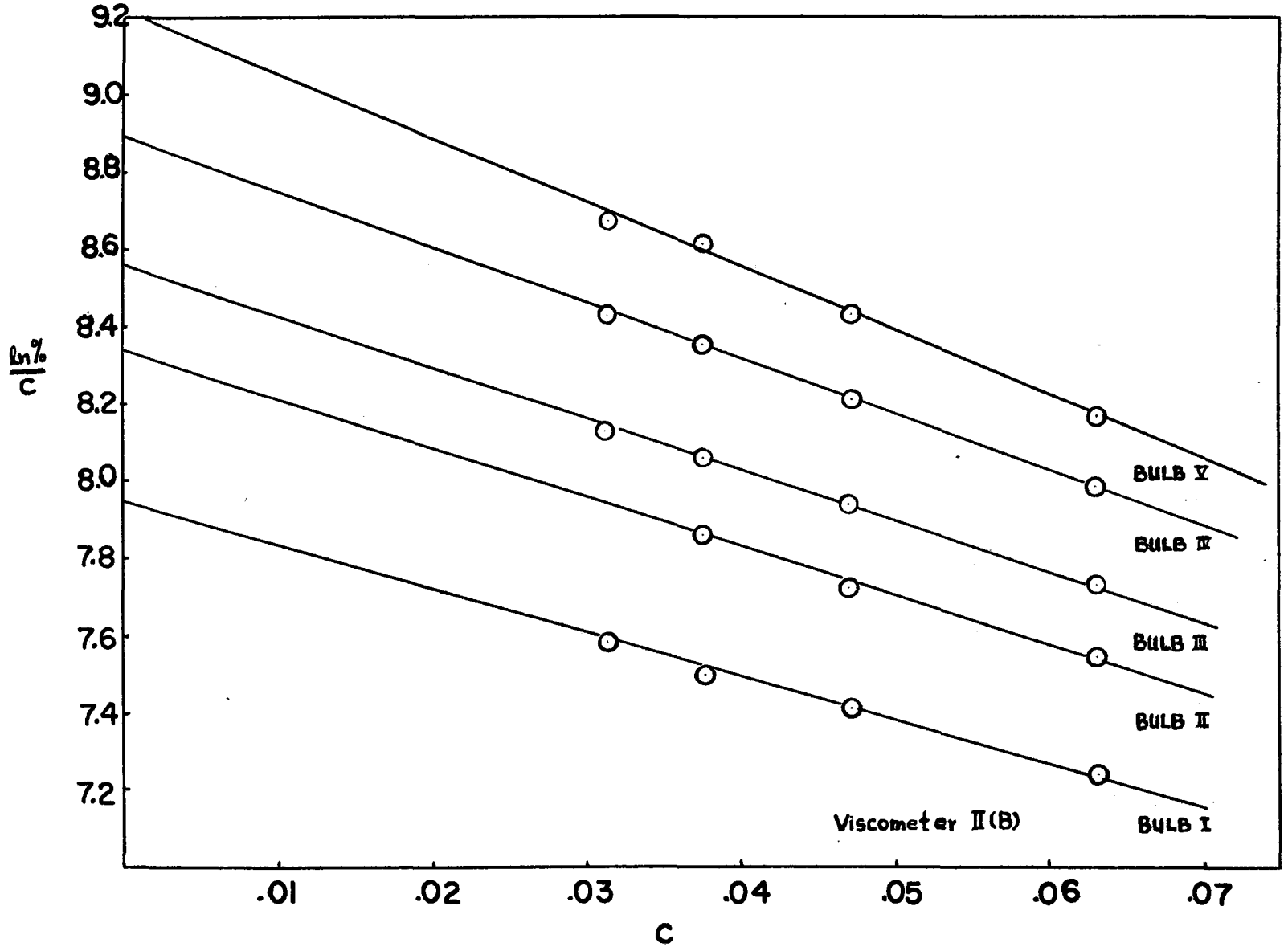

Inherent Viscosity vs Concentration Plot of Polystylene T_5 in Toluene at 20° C

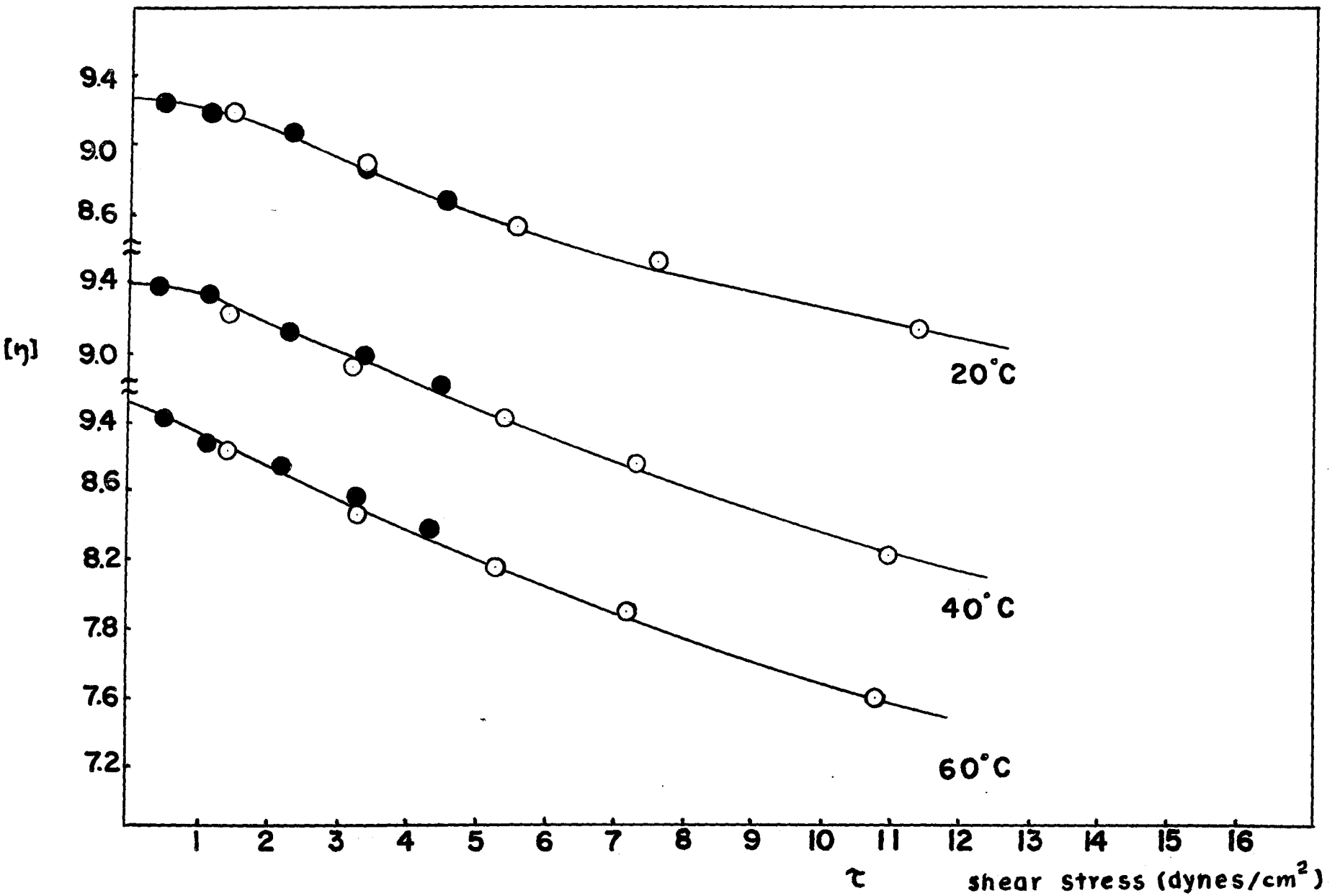

Fig 11

Dependence of the Intrinsic Viscosity on Shear Stress of Polystylene T_5 in Toluene at Various Temperatures

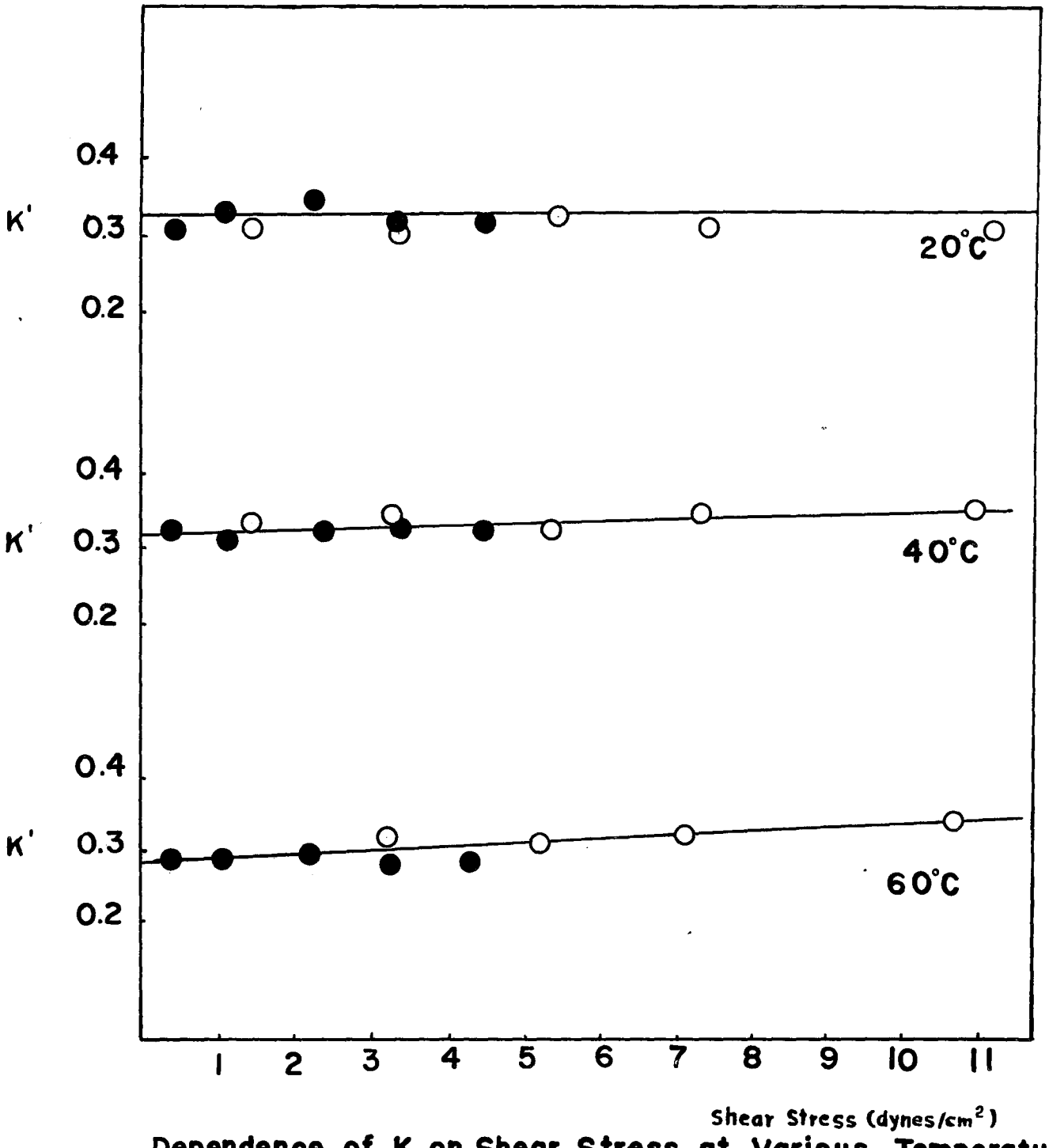

Dependence of K on Shear Stress at Various Temperatures for Polystylene in Toluene

Fig VI